pH-sensitive Anticancer Prodrug: Amide of Kemp's Acid

A thesis

submitted in partial fulfilment

of the requirements of the degree

of

Masters of Science in Chemistry

at

The University of Waikato

by

Robert Turongo Brooks

University of Waikato

2009

THE UNIVERSITY OF
WAIKATO
Te Whare Wānanga o Waikato

Abstract

Solid tumours are characterised by lower extracellular pH (as low as 5.8 pH) compared to normal healthy cellular pH (actively regulated at pH 7.3). This difference may be exploited with an acid-sensitive anti-tumour prodrug which releases a cytotoxin selectively in tumour tissue.

The research reported in this thesis was aimed at synthesising and performing rate studies on an amide prodrug with pH-sensitive rates of reaction in the pH 5 – 8 region. Amide hydrolysis is catalysed by neighbouring carboxylic acid groups in their fully protonated state but not in its ionised state (shown in the figure below), whereby pH sensitivity around pH 5 – 8 can be exploited. The current study was carried out on an amide of Kemp's acid which, due to enforced stereochemistry of carboxylic acid and amide functional groups, has the type of structure conducive to accelerated amide hydrolysis.

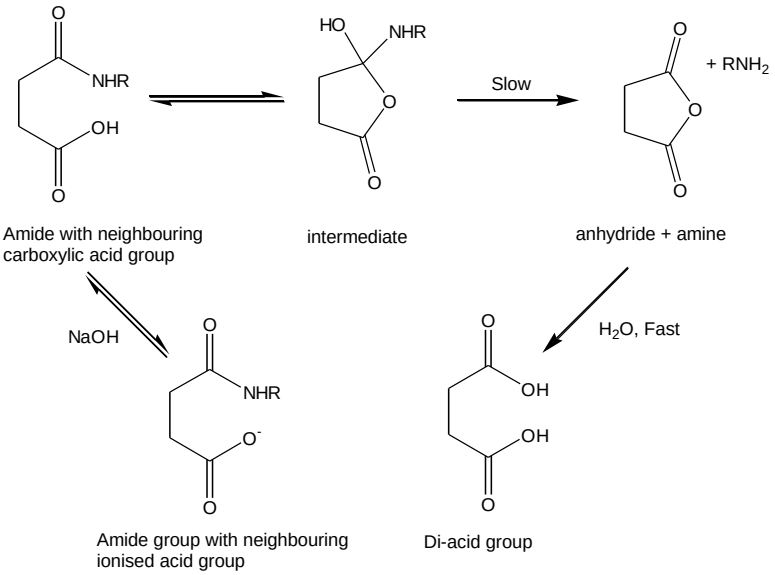

The rates for tertiary and secondary aliphatic amides of this Kemp's acid system have shown high reactivity at low pH and a large reduction in rate across pH 5.8 – 7.3, however an aryl amide had not previously been studied. It was thought that an aryl amide of Kemp's acid would provide a faster rate of reaction compared with the alkyl amides, and also aryl amine cytotoxins exist which could be attached as an amide.

A secondary aryl amide of Kemp's acid **(58)** was obtained via a potassium hydroxide ring-opening reaction on a synthesised imide of Kemp's acid **(43)**.

(58)

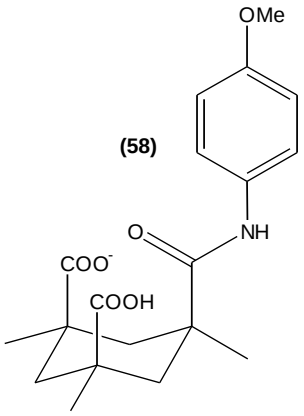

Aliquots of the ring-opened amide **(58)** were added to buffered (phosphate and malonate) aqueous solutions (with ionic strength μ = 1 mol L^{-1}) and the hydrolysis reaction followed at 30.0 ^{o}C across the pH range 0.48 - 8. First order rate constants were calculated from absorbance change with time and the pH-rate profile established. Absorbance changes were shown to be consistent with amide hydrolysis with no evidence of any imide reformation as evident in other studies. The rate data were analysed. There was no evidence from rates for the two successive acid ionisations

with only a single rate plateau evident from pH 2 to 5, suggesting that both di- and mono-acid species have very similar hydrolysis rates or that the second ionisation is low due to stabilisation of the mono-ionised molecule by hydrogen bonding interactions. For this reason, the rate profile could be analysed only as if it were a single ionisation in the same way that Menger and Ladika analysed their aliphatic tertiary pyrrolidyl amide in an earlier study. This analysis gave a pK_a value of 6.72 ± 0.09 and a limiting rate constant of 7.1×10^{-5} s^{-1}. The studies revealed a three fold rate differential between pH 5.8 (faster) versus 7.3 (slower), a difference which is probably too small a selectivity for possible prodrug application.

Separately, the second order rate coefficient for the reaction of potassium hydroxide solution to open the imide was also established (k_2 = 0.00067 L mol^{-1} s^{-1} at 30.0 ^{o}C, μ = 1.00 mol L^{-1} with KCl).

Acknowledgements

First of all, a big thanks must be extended to my supervisor Associate Professor Lyndsay Main, for his seemingly tireless devotion to my plan of research, his approachability even when the questions of were of objectionable quality and his plethora of chemical knowledge.

To everyone in the chemistry department, staff and students, for your help with all things chemical, experimental and conversational, you all have been wonderful in your own way, allowing me to “borrow” things, teaching me new things and keeping my mind intact on a number of occasions.

Also to those people located around the campus who have assisted me in various ways, especially those in Te Ahurutanga for your support and help with scholarships and the nomination for the 2008 aspiring leaders forum.

To all of my loved ones, whānau and friends, your support throughout my five and a half year university career chasing my dreams has been nothing short of awesome, thank you for being there!

Finally, my gratitude must be extended to those businesses, organisations and trusts that have sponsored my study with scholarships and internships, Tainui trust board, AgResearch Ruakura, Ngā Pae o te Māramatanga and the University of Waikato Masters research scholarship.

Table of contents

List of figures

List of tables

Abbreviations

Δ_t – specific time interval

A_∞ - Absorbance at time infinity

A_t – Absorbance at time *t*

AnalaR – Analytical Reagent

BuLi – Butyl Lithium

CBI – cyclopropylbenzidoline

CML – Chronic myeloid leukaemia

DNA – Deoxyribonucleic acid

DCM – Dichloromethane

DMAP – Dimethylaminopyridine

DNR - Daunorubicin

d – Doublet

GIST - Gastrointestinal stromal tumours

IR – Infra-red

J – Coupling constant

k_{obs} – Observed first order rate constant

MAb – Monoclonal Antibody

μ - Ionic strength

NMR- Nuclear Magnetic Resonance

s – Singlet

Σ – Sum of

t – Triplet

$t_{1/2}$ – Half-life

TAP – Tumour Activated Prodrug

UV - Ultra-Violet

Vis - Visible light range

λ_{max} – Wavelength of maximum absorbance

1 Introduction

1.1 What is cancer?

Cancer is a collective term used for a group of diseases where cells lose the ability to undergo *apoptosis* (cellular programmed death) resulting in unregulated cellular division. Cancerous tumours generally have three properties that separate them from benign tumours:

- Uncontrolled cellular replication
- Invasion - Where rapidly proliferating cells invade surrounding tissues
- Metastasis – Spread of the cancer throughout the body via the blood and lymph systems[1]

Cancer can affect both animals and plants, and in humans is responsible for approximately 13% of all deaths worldwide.[2] It can affect people of all ages, though the risk for most forms of cancer increases with age and is more prevalent in developed countries where life expectancy is higher.[2, 3] Cancers typically take the form of solid tumours or carcinomas, which arise from epithelial cells and account for 80-90% of all cancers, but can also take other forms, such as:

- Sarcoma – Cancerous tumour originating in the bone, cartilage, muscle, fibrous connective tissue or fatty tissue
- Myeloma – Cancerous tumour originating in the plasma cells of the bone marrow

- Lymphoma – Cancerous tumour originating in the lymph system
- Leukaemia – Cancer originating in the blood-forming tissue[4]

It is widely documented that cancers arise from evolution within a cellular population of the body.[5-7] This evolution occurs due to genetic errors that are accumulated throughout a cell's life span which causes irreversible errors in the genetic makeup of the cell, eventually allowing the cell to be free of apoptosis. Errors occur during the replication of DNA, but there are mechanisms to prevent cellular division in cases where the genome may be extensively compromised, and failure to arrest this development leads to the formation of cells with highly unstable genomes that may become neoplastic (part of an abnormal mass of tissue), and could possibly go on to become malignant.[8]

These mechanisms include the activity of enzymes such as DNA polymerase which helps to rectify any mistakes that are made to the genetic code during DNA replication. Apoptosis is another mechanism, where DNA-degrading nucleases are unleashed in the cell, destroying the cell's ability to divide. Apoptosis occurs when a cell is damaged beyond repair, infected with a virus or is in a stressful environment such as starvation.[8]

Even with these correction mechanisms in place, errors still do occur and are passed onto subsequent generations of cells. Some of these mutations may cause a cell to become neoplastic, providing it with an advantage over surrounding cells in that it may be able to replicate faster

or more efficiently, thus producing a subpopulation of a new predominant cell.[5] Progressively more mutations may arise in further generations of daughter cells, compounding these initial errors and eventually leading to a cell that acts contrary to its intended function in the animal. In this regard, cancer is a progressive disease, where errors slowly accumulate in a cellular population to a point where a cell may become “immortal” such that it is free from apoptosis and can rapidly divide, resulting in the six “hallmarks of cancer”:

- Self sufficiency of cells in signals controlling growth
- Loss of sensitivity to antigrowth signals
- Evasion of apoptosis via mutation or loss of tumour suppressor genes
- Development of limitless replicative potential, usually via the expression of telomerase
- Sustained angiogenesis, whereby the blood supply to a tumour is augmented
- Tissue invasion and metastasis, which causes 90% of all cancer-related deaths.[9]

1.1.1 Causes of cancer

As discussed previously, cancer occurs through acquired genetic mutations. There are some areas in the body where there are greater risks of mutations and thus a greater risk of cancer. These are areas where

cells that are constantly replicating and have high exposure levels to carcinogens. The most well documented source of chemical carcinogens is tobacco smoke, which has been linked to the incidence of over 90% of all lung cancers[10, 11] and also to cancers of the paranasal sinuses, stomach, liver, kidney and uterine cervix.[12] Another is asbestos, with prolonged inhalation of asbestos fibres linked with development of the lung cancer mesothelioma.[13] These carcinogens have a mutagenic effect on the genetic material in cells, raising the likelihood of acquiring the mutations that cause them to become malignant. Non-chemical carcinogens, such as ionising radiation, can also cause mutations to the genetic material of a cell. The most well-known type of ionizing radiation is high energy ultraviolet light (UV) originating from the sun. High levels of exposure to UV radiation have been known to result in high incidence of melanomas and other types of skin cancers.[14]

It has become increasingly evident that viral infections also play a role in the development of cancers, with up to 20% of all cancers worldwide stemming from viral infection.[15] It is thought that viral infection causes insertion of viral DNA into the genome of the host which encodes for oncogenes or causes the up-regulation of oncogenes, resulting in a higher chance of developing cancer.[15] One such virus is human papillomavirus, which worldwide is the cause of greater than 93% of invasive cervical cancer cases in women[16] as well as hepatitis B and hepatitis C which have been linked to hepatocellular carcinoma (malignancy of the liver).[15]

Cells that have a high turnover rate have a higher risk of mutations because the cellular machinery in place to repair errors made during DNA replication is more likely to miss or incompletely repair errors, leading to mutations being passed on to daughter cells.

There are specific genes that become suppressed or expressed at higher levels than usual, which are known to affect the occurrence of specific cancers. There are two broad groups that encompass the two types of genes: oncogenes and tumour suppressor genes. Oncogenes are genes that, when expressed at high levels, promote the formation of a cancerous cell,[17] whilst tumour suppressor genes suppress the formation of a mutation that could predispose a cell towards malignancy. A genetic mutation may deactivate a suppressor gene such that it cannot have this effect. A classic example of this is the tumour suppressor gene p53. This gene was found to play a large role in the suppression of tumours via its regulatory role in the cellular cycle.[18] Its main means of preventing the onset of tumours is preventing genomic mutation by inducing cell cycle arrest in response to DNA damage.[19] Studies with transgenic mice without the p53 gene were prone to spontaneous development of tumours at a very early stage of life.[20]

1.2 Treatment methods for cancer

There is currently a wide range of methods for treating cancer, from non-discriminatory methods such as radiation therapy down to highly specific

methods of treatment such as immunotherapy. Surgery is often used to remove tumourous tissue in conjunction with one or more of these techniques. The main methods of non-invasive cancer treatment are as follows.

1.2.1 Radiation therapy

Radiation therapy is a method of treating solid tumours which utilises ionising radiation to kill cancer cells. Treatment involves targeting a specified area of the body with high energy ionising radiation, which damages the genetic material in cells, rendering them incapable of cellular division. Total body irradiation is also possible, but as the treatment is not selective. Cells surrounding a tumour target will also be damaged leading to an increased chance of those cells developing malignancy in later life.

1.2.2 Chemotherapy

Chemotherapy is the use of chemicals to treat or control cancer using cytotoxic compounds that destroy cancer cells by interfering with their growth or preventing their reproduction.[4] They work by interrupting the cell cycle at specific stages (depending on the drug) and arrest cellular division. Chemotherapy treatments are generally more effective against rapidly dividing cells, making cancer cells more susceptible as they typically undergo rapid cellular division. However, normal body cells can also be damaged, with the damaged cells typically being dividing cells such as hair cells, bone marrow cells and the cells lining the intestine and mouth.

This leads to hair loss, mouth and stomach ulcers, as well as bone marrow depletion which can cause immune system depression. There are many different chemotherapy agents, each targeting a different aspect of the cell cycle such as: alkylating agents, antimetabolites, plant alkaloids, vinca alkaloids and topoisomerase inhibitors. Often, a course of treatment will require a combination of several drugs from these different classes to try and affect as many stages of the cell cycle as possible.[4]

1.2.3 Newer methods

Newer methods of cancer treatment include hormonal therapy, immunotherapy and targeted therapy, all of which work by targeting small but significant differences between tumour tissue and healthy tissue. Targeted therapy is designed to interfere with a specific molecular target that is believed to have a critical role in tumour growth and development.[21] The drug imatinib mesylate (marketed as Gleevec) specifically inhibits tyrosine kinase enzymes, making it highly effective against chronic myeloid leukaemia (CML) and gastrointestinal stromal tumours (GIST). This is because CML is caused by a mutant kinase fusion protein Bcr-Abl, and GIST is caused by either point mutations in the cytokine receptor c-Kit or platelet derived growth factor receptor – α kinases. Imatinib effectively inhibits all three kinases halting progression of the cancer, with almost no effect on healthy cells. However, this type of treatment is highly specialised, and is only effective against a small number of cancers.[21]

Another drug that targets a specific mechanism is angiogenesis inhibitors, which inhibit the development of new blood vessels. New blood vessel development is necessary for the growth and development of a tumour.[22] These new blood vessels are the primary route of nutrient introduction into a tumour and also the primary route that tumour cells exit and metastasise throughout the body.[23] Typically, new blood vessel development only occurs in growing and healing tissue, so in a normal adult this blood vessel development is limited to growing tumour tissue allowing inhibiting drugs to prevent the growth of a tumour, whilst not effecting healthy tissue, by targeting a major difference between tumour tissue and normal healthy tissue.

1.3 Differences between tumour tissue and healthy tissue

1.3.1 Hypoxia

Due to the highly disorganised method of blood capillary development in tumours there are a significant number of tumour cells that are too far away from blood capillaries to allow proper oxygen diffusion into the tissue. This leads to these cells becoming hypoxic either temporarily or permanently. This was postulated in 1955 by Thomlinson and Gray[24] as a difference between tumour tissue and healthy tissue. Normal cancer treatment methods are sometimes ineffective against hypoxic regions, as they are located too far away from blood vessels for adequate diffusion of anti-cancer drugs. Because oxygen acts as a radiosensitiser, radiation

treatment is less effective against hypoxic tumour cells[25], making them two to three times more resistant to radiation than those in a non-hypoxic environment.[26] But because of the difference in oxygen levels that are unique to tumour tissue, these hypoxic regions can be targeted by prodrugs for anticancer therapies.[3,27]

1.3.2 Increased extracellular pH

Due to disorganised blood capillary development in large tumours, the pH is lower than that of surrounding healthy tissue. This is thought to be caused by inefficient clearance of acidic metabolic products from chronically hypoxic cells which cause the extracellular pH (pH_e) to be lower than pH 6.3 and as low as pH 5.8[28], compared to normal pH inside cells (pH_i) which is actively regulated at pH 7.3.[27, 29] This is one of the few well-documented differences between cancer tissue and healthy tissue.[30] Although the magnitude of this pH difference is small it is possible to design prodrugs which have higher rates of reaction at the lower pH of 6.3 than at normal intracellular pH of 7.3. To date there has been relatively little work done on exploiting this small pH difference as it is difficult to find molecules that have a sufficiently large rate differential at pH 6.3 vs. pH 7.3. Examples of systems that have been studied will be discussed in **section 1.4**

1.4 Prodrugs and studies on possible prodrug systems

Whilst the methods outlined in the previous section (**section 1.2**) on cancer treatment methods show that the methods can be successful in treating cancer, it can also be seen that there is a large number of disadvantages of these methods, such as lack of selectivity for cancer cells, physiological effects and resistance to the treatment method. In all likelihood a universal treatment of all solid tumours is doubtful, however, a possible answer to these problems lies in designing drugs which target differences between cancerous tissue and healthy tissue.

Drugs that perform this task, such as the Gleevec example mentioned previously (**section 1.2.3**), have the disadvantage of specificity, that is to say they are too specific for use other than against the hormone or enzyme they are designed to inhibit. So while they work well for these specific cases, the chances of being able to utilise drugs such as Gleevec in other anti-cancer scenarios is small. Designing drugs to target less specific differences such as hypoxia and pH shows promise, as these two differences are unique to tumours.

An example of drugs being used to target these differences are prodrugs. The term prodrug was first coined by Albert[31] and is a medicine that is administered in an inactive form and is metabolised *in vivo* into an active product. In this broader definition, the clinical drug codeine is a common example of a prodrug, as it is demethylated by the liver enzyme CYP2D6 to morphine. However, for the purposes of this thesis, the interest is in

prodrugs that are activated in tumours for anticancer purposes. There has been a large amount of interest in these tumour-activated prodrugs (TAP)[27] because of their potential to release a cytotoxin in conditions prevalent in tumours such as hypoxia and lower extracellular pH. In this scenario a prodrug would be inactive in the blood stream but upon release into a tumour site, be converted into an active cytotoxin with the aim of killing the cancerous cells.

Denny[32] proposed a theoretical prodrug structure (**Figure 1-1**) which includes a trigger unit attached to the effector unit (which can be visualised as the cytotoxin) via a linker unit.

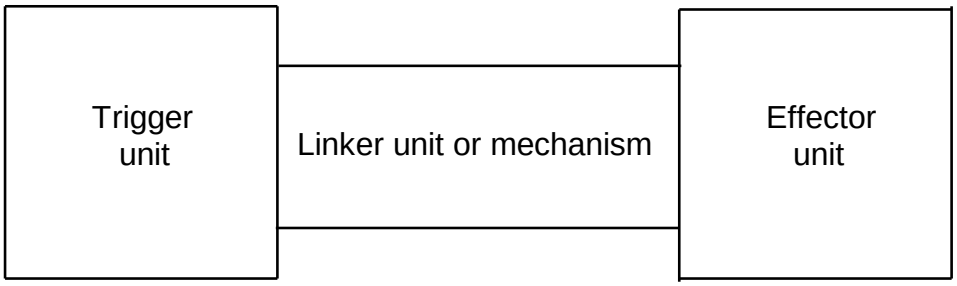

Figure 1-1: Model for prodrug design as proposed by Denny[32]

1.4.1 Advantages of prodrugs

An obvious advantage of prodrugs over other antiproliferative agents is selectivity. Antiproliferative agents such as *cis*-platin are effective but are limited in their use due to their toxic effects on healthy cells. This is because these classes of drugs do not target fundamental changes in cancerous cells, but rather changes that occur after these fundamental changes, for example rapid cellular division. An advantage of prodrugs is

the ability to alter the structure of the prodrug to modify the overall pharmacological properties without jeopardising the effectiveness of the drug. Because the activation step is the step of primary selectivity, the selectivity of the cytotoxin is of lesser concern, and can be chosen from simple cytotoxicity tests to be as potent as possible.

1.4.2 Types of prodrugs

There are several types of prodrug designs, with each design corresponding to a particular set of tumour conditions that would allow release of a cytotoxin[27]:

i. Tumour hypoxia

ii. Selective enzyme expression in tumour cells (also other enzyme targeted therapies such as ADEPT and GDEPT)

iii. Radiotherapy

iv. Tumour specific antigens

v. Lower extracellular pH

As the research summarised in this thesis is concerned only with synthesis of a pH activated prodrug, discussion of prodrugs will centre on this area of research.

1.4.3 Prodrugs activated by pH differences

As discussed in **section 1.3.1** the disorganised blood capillary development in rapidly growing tumours causes regions of low extracellular pH. The reason for this low pH is that metabolic by-products in chronically hypoxic regions cannot be extracted by the bloodstream. The pH difference between normal tissue and tumour tissue can be up to 0.8 pH[30] and the extracellular pH of a tumour as low as 5.8.[28] This is a small but significant difference, which can be used as a target for prodrug therapies. One mechanism of activation of this type of prodrug would be to increase breakdown of the prodrugs at this lower pH found in tumour sites. Drugs with this capacity would have the following advantages:

- Because the activation is non-enzymatic, it would not require the presence of suitable activating enzyme systems which may only be present in small amounts or at certain stages of the cellular life-cycle

- As the activation process is extracellular, the prodrug would be designed to be excluded from cells, assisting its diffusion into the tumour and also contributing to a large difference in toxicity between the prodrug in its non-activated and activated forms.[32]

However, due to the small difference between pH_i and pH_e, relatively little work has been done on prodrugs sensitive to this pH difference. Studies that have been conducted on systems with potential for pH activated

release have yielded few compounds with sufficiently large differences in hydrolysis rates in this small pH range.

The rest of this introduction will examine some studies conducted on potential pH-sensitive prodrug systems and the potential for further analysis on some of these systems, more specifically on the Kemp's acid molecule.

1.4.4 Gentamicin system

An example of a prodrug system is one patented by Eilat and Arad-Yellin (2000).[33] Their study involved attaching the Gentamicin drug to an acid-cleavable linkage molecule **(3, Figure 1-3)**. At lower pH this linker group cyclises and releases the cytotoxic Gentamicin (**Figure 1-2**). After being dissolved in pH 6.5 buffer for 24 hours, NMR spectral studies on the system showed that 25% of the linker molecules **(1)** had been hydrolysed to **(2)** and so released Gentamicin. The same test for a pH 6 buffer showed a 40% hydrolysis rate. In a far more acidic medium (pH = 1), more than 90% of the linker molecules were hydrolysed to release Gentamicin after 24 hours.

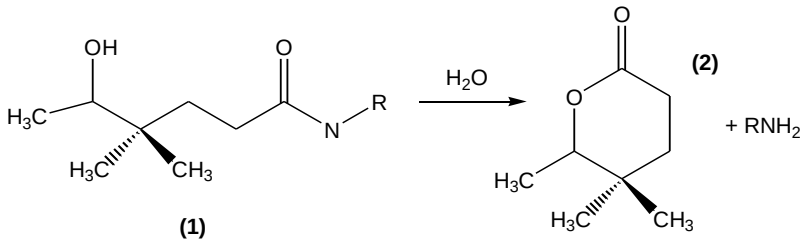

Figure 1-2: pH-sensitive linker group from Eilat patent[33]

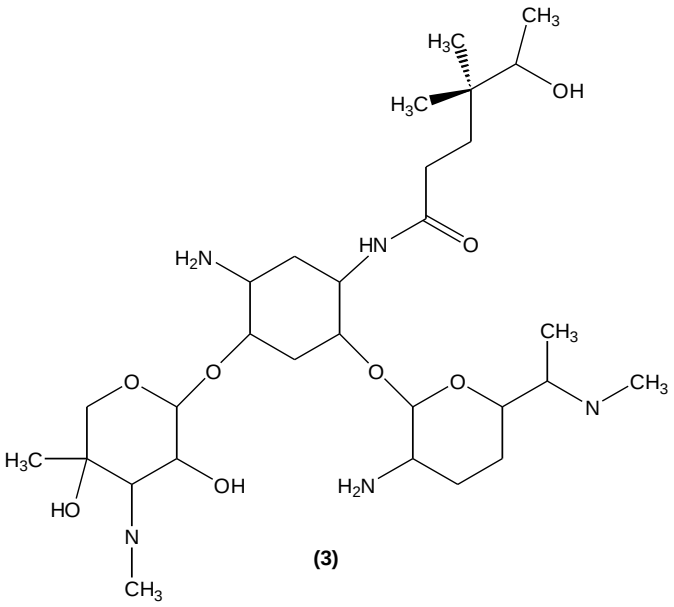

(3)

Figure 1-3: Gentamicin – pH sensitive linker system[33]

1.4.5 Glucoside acetal prodrug

Based on findings that the pH in tumour cells can be decreased by stimulation of aerobic glycolysis,[34] a glucoside acetal prodrug **(6)** was synthesised. The mechanism for formation of **(8)** is hydrolysis of **(4)** to yield **(5)** and **(6)**. The phosphoramide mustard **(8)** is produced through breakdown of the released aldehyde **(6)**, with release of the ester group **(7)** **(Figure 1-4)**. Studying the cytotoxicity of **(6)** in cultured rat mammary carcinoma cells showed that the molecule exhibited little toxicity at pH 7.4, but when the environmental pH was lowered to 6.2-5.6 pH, **(6)** exhibited dose-dependent cytotoxicity.

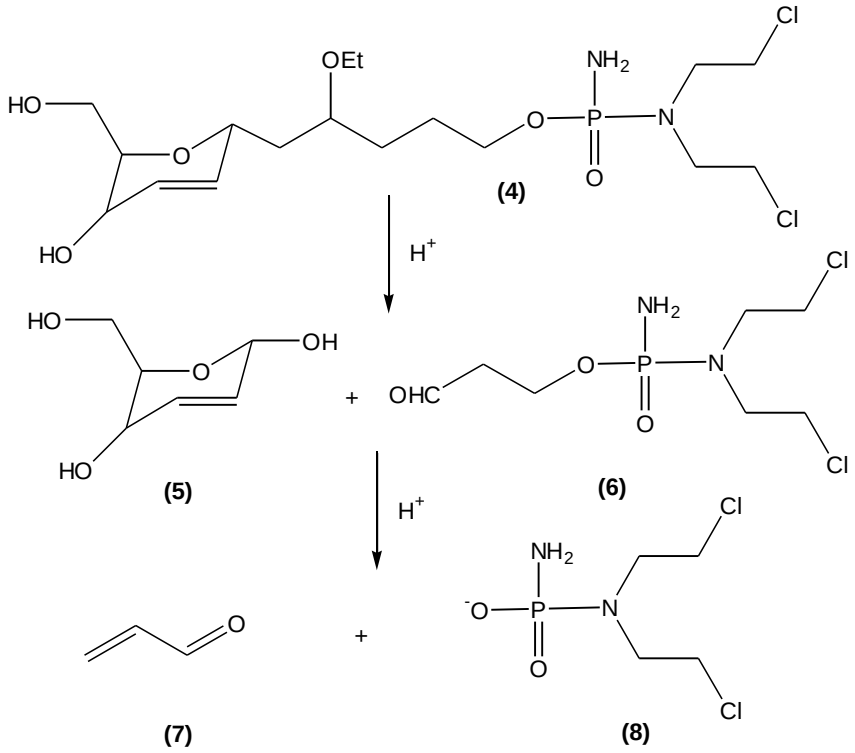

Figure 1-4: Mechanism for preparation of glucoside prodrug **(6)** and subsequent breakdown to a phosphoramide mustard **(8)**[34]

1.4.6 Amide and carboxylic acid systems

A number of studies that have been conducted have been centred on carboxylic acid-amide related systems, as this makes use of the phenomenon that amides undergo accelerated hydrolysis with neighbouring carboxylic acid groups **(Figure 1-5)**. In this basic mechanism, intramolecular attack occurs by the carboxylic acid group on the amide in **(9)** group which reacts to from an anhydride and amine **(11)** which is the model for the cytotoxin. When the carboxylate group is ionised at higher pH, no intramolecular attack occurs so no amine is released **(12)**. Therefore this reaction has the potential to be faster at tumour pH than at

normal tissue pH. The scheme illustrated show a 4-membered carbon chain which cyclises to form the 4-membered carbon cyclic structure. The purpose of the linker unit is to enforce proximity upon the functional groups that react to release the amine **(11)** to ensure rapid intramolecular reaction.

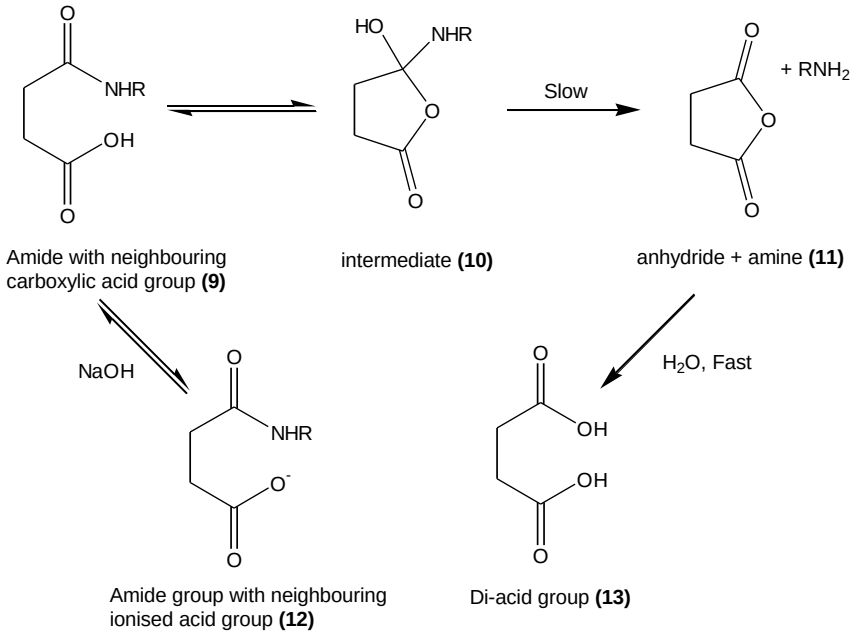

Figure 1-5: Scheme for hydrolysis reaction of an amide by a neighbouring carboxylic acid group

1.4.7 Bicyclic carboxyamides

Bicyclic carboxyamides are a new class of amides originally studied and characterised by Glusenkamp and colleagues[35] in 1998. The aim of their study was to construct models for new prodrug systems that contained tailor-made acid-labile protective groups for pH related activation to be used in cancer therapy applications. A wide range of amides were created (**Figure 1-6**, **Table 1-1**) with substituents that would have a major influence on the acid lability of the amide bond (formed synthetically for

the study between an amine and an anhydride **(14)**). In order to maximise the amount of structural variety, highly substituted bicyclic anhydrides were chosen as precursors to the acid labile amides. **Figure 1-6** shows the bicyclic anhydride **(14)** and its corresponding *N*-methyl tryptamine derivatives **(14a).** All the tertiary amides synthesised were hydrolysed in aqueous buffer solution at various pHs to determine their respective half-lives (**Table 1-2**).

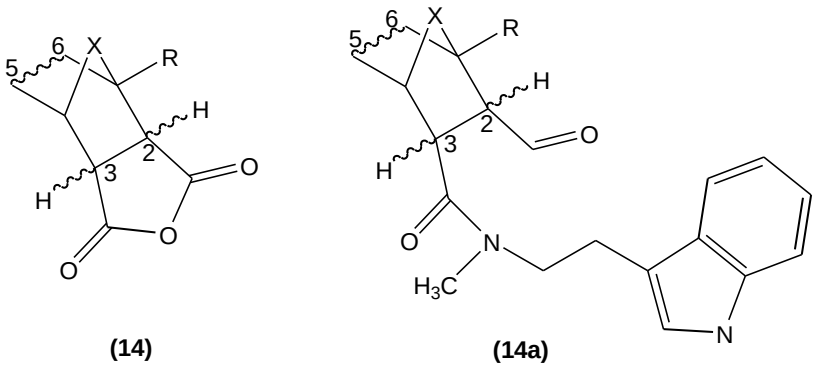

Figure 1-6: Bicyclic anhydrides **(14)** and amides **(14a)** synthesised by Glusenkamp *et al*[35]

Table 1-1: Substituents at R and X positions

Compound	X	R
14, 14a	O	CH_2-O-COPh; 2,3-exo; 5,6-CH
15, 15a	O	CH_2-O-COPh; 2,3-exo; 5,6-CH_2
16, 16a	O	CH_2-O-COPh; 2,3-endo; 5,6-CH
17,17a	O	CH_2-O-COPh; 2,3-endo; 5,6-CH_2
18, 18a	O	H; 2,3-exo; 5,6-CH
19, 19a	O	H; 2,3-exo; 5,6-CH_2
20, 20a	CH_2	H; 2,3-endo; 5,6-CH
21, 21a	CH_2	H; 2,3-endo; 5,6-CH_2
22, 22a	CH_2-CH_2	H; 5,6-CH_2

Table 1-2: Cleavage rates of the *N*-methyl-tryptamine adducts **14a - 22a**

Compound	$pK_{(app)}$	$t_{1/2}$ at pH 5 (minutes)	$t_{1/2}$ at pH 6 (minutes)	$t_{1/2}$ at pH 7 (hours)
14a	4.6	67	336	39
15a	4.6	17	106	14
16a	4.7	312	1560	208
17a	4.5	155	930	124
18a	4.5	31	159	21
19a	4.6	10	52	7
20a	5.4	2	13	1.7
21a	5.4	2	13	1.7
22a	5.9	0.3	0.5	0.04

From these data, it can be seen that all amides display much smaller cleavage half-lives at pH 5 than at pH 6 and these than at pH 7. Molecules with the CH_2 group at the X position showed the smallest half-lives, with molecule **(22a)** showing a half-life of 2.6 minutes at pH 7. Molecules **(20a)** and **(21a)**, which are endo, show slightly slower $t_{1/2}$. Those with oxygen at the bridging X position have longer half-lives with the exo isomers having the shorter half-lives; however the endo isomers show the smallest half-lives with CH_2 as the bridging group. The reasons for these differences are not explored in the published paper other than stating that that a 0.15 Å difference in distance from the acid carbonyl carbon to the adjacent amide carbonyl carbon is responsible for the difference in reactivity between **(22a)** (2.79 Å) and **(16a)** (2.94 Å). A possible reason for the difference in reactivity with oxygen as the bridging group is the rigid stereochemistry of

the functional groups at carbon positions 2 and 3. Overall this study showed it was possible to synthesise a wide variety of structures, all showing decreased activity at pH 7 compared to the lower pHs of 5 and 6. The molecules that have the oxygen bridge (specifically those with exo isomer) show more promise with respect to prodrug application as they have half-lives at pH 6 that would allow them to activate preferentially in a tumour.

1.4.8 Maleic amides

It is known that amides of maleic acid undergo hydrolysis in their neutral form to form maleic anhydride and release amine in a method akin to that shown in (**Figure 1-5**), although for an ionised maleic acid hydrolysis occurs albeit slowly. This leads to a plateau in the pH rate profile below pH 3, with the pK_a being approximately 3.5. Although this is too low for any potential prodrug application, the rates of reaction for this compound can be increased by the modification of groups on the double bond. An example of this is a Daunorubicin (DNR) conjugate system synthesised and studied by Dillman *et al* (**Figure 1-7**).[36] This system involved the attachment of the anticancer agent Daunorubicin and the monoclonal antibody T101 to a maleic acid amide which acts as an acid-sensitive linker group between the two. Tests were done measuring absorption (475 nm, for free DNR) in buffer solutions at 37 ^{o}C (with incubation periods of one, two, four, 24 and 48 hours) at pH 3, 4, 5, 6, 7 and 8.

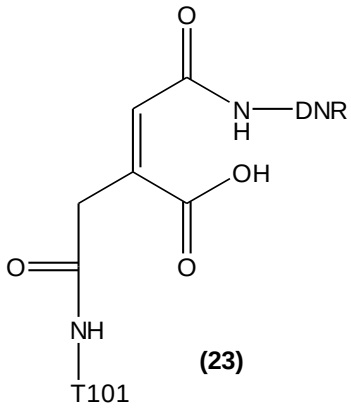

(23)

Figure 1-7: Daunorubicin (DNR) - maleic acid amide – T101 Monoclonal Antibody conjugate[36]

The highest absorptions were seen at pH 3 and 4, corresponding to nearly 100% drug release, with absorption decreasing to nearly zero for solutions at pH 7 and 8 (0% release), while at ph 5 there was roughly 50% release, thus confirming the pH sensitivity of this compound. Also studied was the difference in anti-tumour effect of the conjugate compared to the free Daunorubicin drug. This experiment was conducted in athymic mice bearing human tumour xenografts (MOLT-4 cell-line). The experiment was designed to test the effectiveness of the two systems on tumour size. The mice were treated with equal doses of the conjugate DNR-maleic amide-T101a system **(23)**, DNR-T101 and DNR by itself. The conjugate system showed vastly decreased tumour size relative to the stand-alone Daunorubicin drug.

1.4.9 Cyclopentane tetracarboxylic acid amide

Cyclopentane systems with four all-*cis* carboxylic acid groups were studied by Billett and colleagues[37] with the intention of finding the potential of such

systems for prodrug use. Studies with this system were initiated as the problem with the mechanism in **Figure 1-5** is that hydrolysis slows with increasing pH, as the amount of the non-reactive conjugate base **(12)** increases; with pK_a values of carboxylic acids seldom being above 4.5, monocarboxylic acids are nearly completely ionised below pH 5.5 and rates of amide hydrolysis become low tending towards neutral pH as the amount of neighbouring carboxylic acid group in a catalytic free form decreases. However three carboxylic acid groups elsewhere in the amide structure raise the second and third pK_a and ensure that close to pH 7 there are still available some undissociated COOH groups to react intramolecularly to form the intermediate **(24)**.[37]

Two diacid imides were synthesised **(25a, 25b)** (**Figure 1-8**) to test the rate of reactions of the compounds at pD 5–7 in aqueous D_2O buffer. The amides were formed by ring-opening of the imides with NaOD and then neutralisation. Analysing the reaction of the tri-acid amide **(24)** by NMR showed that the major product of the reaction was the imide product **(25a)**, whilst the sought after hydrolysis reaction that releases amine **(26)** was minor (an example of one of the studied reactions is shown in **Figure 1-9**). This thwarted the possibility of prodrug applicability of these cyclopentane systems.

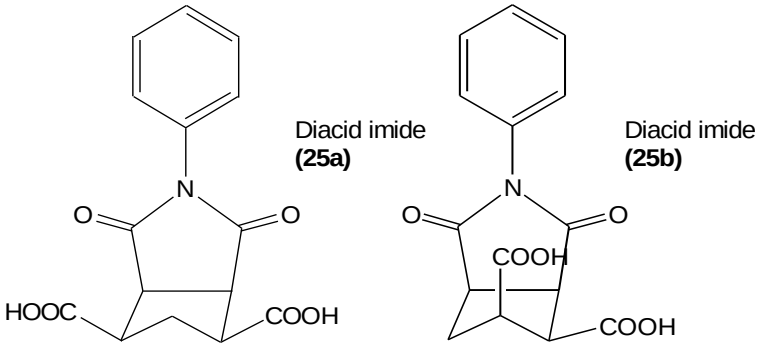

Figure 1-8:The two diacid imides synthesised by Billet *et al*[37]

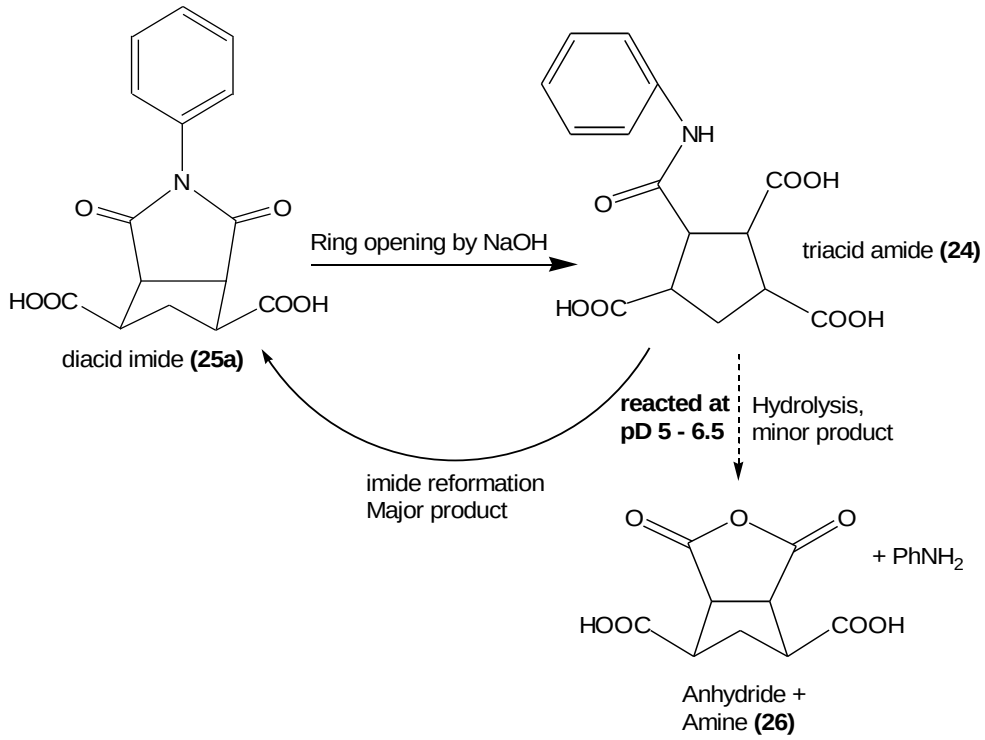

Figure 1-9: Imide reformation as the major product as opposed to hydrolysis for imide **(25a)**[37]

1.5 Kemp's acid

Kemp's acid (*cis,cis*-1,3,5-trimethylcyclohexane-1,3,5-tricarboxylic acid) **(27, Figure 1-10)** was initially synthesised and characterised by Kemp and

Petrakis (in the all *cis* conformation).[38] The interest in prodrug potential for this compound comes from the enforced proximity of the three acid groups which occurs as the methyl groups on the molecule prefer to stay in the equatorial position which is its preferred conformation, proven by x-ray analysis.[39] Flipping into the other chair conformation has been reported[40] for a di-aryl amide Kemp's acid compound.

Important for acid-sensitive prodrug application is the presence of the two carboxylic acid groups in a mono-amide derivative which would ensure that at a pH around pH_e, there would be sufficient unionised acid groups available to promote facile hydrolysis of the amide to form anhydride and amine; but rate would die off with increasing pH as the second acid group ionised. Herein exists potential pH-sensitivity in the pH_e zone. At low pH the diacid would not be ionised at all so individual rates of the neutral, mono- and di-ionised species would determine a composite pH-rate profile.

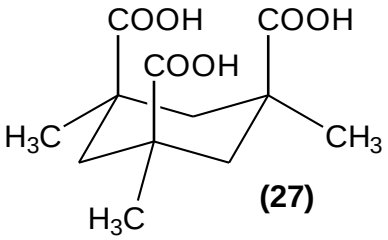

(27)

Figure 1-10: Kemp's acid in the *cis,cis* conformation

1.5.1 Studies on reaction rates and structural effects on reaction rates

Previous studies support the above potential for the amide hydrolysis reaction, as this reaction has been shown to occur quickly at neutral pH and also show a large pH-based differential in rate for some aliphatic tertiary and secondary amides.

Menger and Ladika[41] conducted a study on the rate of intramolecular-catalysed cleavage of an aliphatic tertiary (pyrrolidyl) amide under biological conditions (ambient temperature of 21.5 ^{o}C, neutral pH) in an attempt to find a model for the rapid cleavage of peptide amide bonds exhibited by the enzyme peptidase. Starting for convenience with the anhydride **(28)** in D_2O they monitored the formation of **(29)** and from it **(30)** by NMR spectroscopy (**Figure 1-11**), both reactions as a function of pH. k_1 was larger and it increasingly diverged from k_2 as pD was reduced from 9. This study showed that that the amide cleavage of **(29)** to yield **(30)** occurs with a $t_{1/2}$ of eight minutes at pH 6.9 at which pH, from a calculated pK_a of 6.9, **(29)** would be approximately 50% in mono and di-ionised state**.**

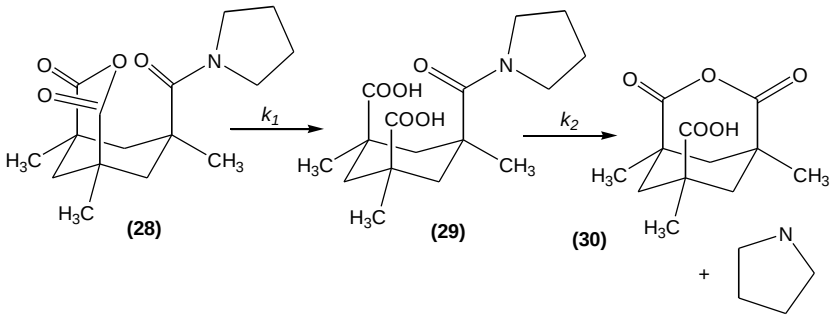

Figure 1-11: Acylolysis reaction studied by Menger and Ladika[41]

Diacid amide **(29)** was assumed to be the active species as the extremely fast rate of reaction was suggested as possibly due to the conformation of **(29)**. Molecular mechanic calculations showed that an interaction that may play a large role in this observed rate of reaction is the distance between the amide carbonyl carbon and the acid hydroxyl group which is 2.80 Å (**(29b) Figure 1-12**). In both situations, there is an almost ideal Dunitz "attack angle" ($O_a/C_b/O_c$ (**Figure 1-12**)) of 105°.[42] Also, the carboxyl group is positioned well for synchronous nucleophilic attack and proton delivery. Another intramolecular distance that could affect the reactivity is the distance between the amide carbonyl carbon and the acid carbonyl carbon, with the distance being 2.78 Å (**(29a) Figure 1-12**).

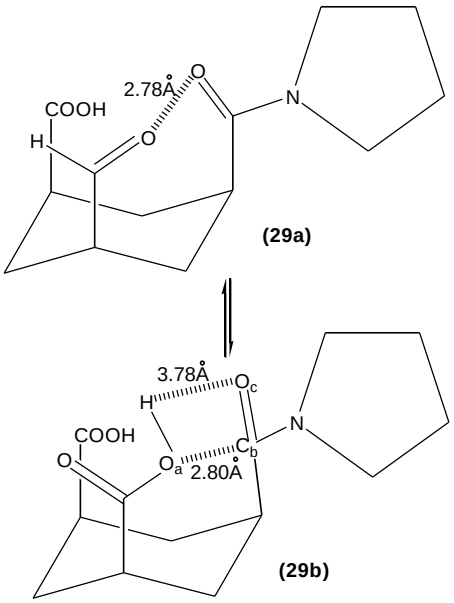

Figure 1-12: Intramolecular distances between adjacent carbonyl groups showing movement around C3-C3' bond (calculated using MACROMODEL)[41]

Full rate profiles for both k_1 and k_2 were determined, with amide cleavage occurring much faster than anhydride hydrolysis (k_2/k_1 = 150 at pD = 7.05, 21.5 ^{o}C). Also discovered in this study was that for the small half-life illustrated above, only one of the carboxyl groups is needed to participate in the amide cleavage. This was established by synthesising an acid-amide-ester **(31)** which underwent amide cleavage rather than ester cleavage (**Figure 1-13**), with a $t_{1/2}$ = 5 minutes (pD = 6.3, 21.5 ^{o}C), which compares well with the half-life for a diacid amide.

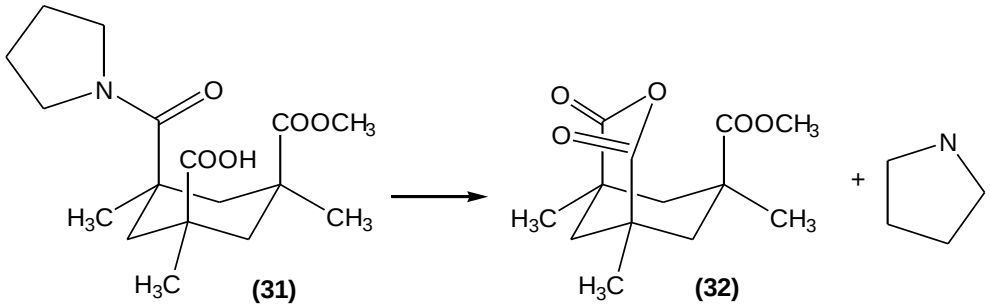

Figure 1-13: Acid-amide-ester hydrolysis reaction

Building upon the research conducted by Menger and Ladika was a study by Curran *et al*[43] comparing the acylolysis rates of secondary and tertiary aryl amides of Kemp's acid (**Figure 1-14**). This study established that the rate constant for acylolysis in D_2O at pD 7 for the tertiary amide derivative **(33a)** of Kemp's acid was 1000 times higher than that for a corresponding secondary amide **(33b)**. The half-life of the synthesised tertiary amide was very similar to that reported by Menger and Ladika, with $t_{1/2}$ = 5.3 min (pD = 7, 22 ^{o}C).

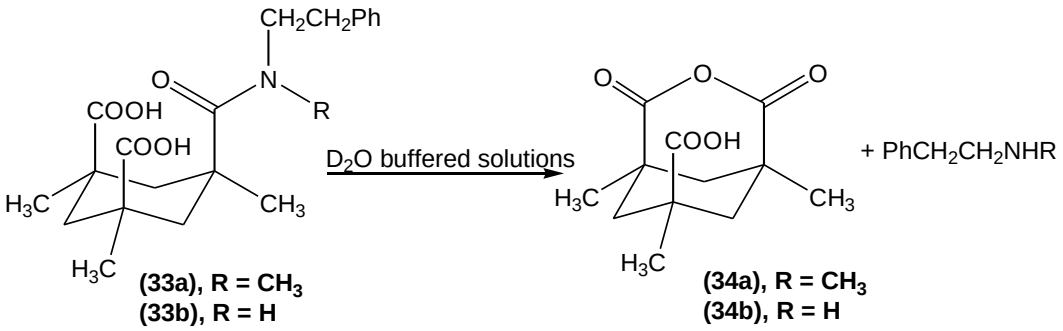

Figure 1-14: Acylolysis of a tertiary amide (R = CH_3) versus a secondary amide (R = H)[43]

A pH rate profile from pD 4 - 9 was plotted to compare the acylolysis rates of the tertiary and secondary amide. This showed that **(33a)** has reaction rates between two to four fold faster than **(33b)** over the entire pD range. For example at pD 4.8 (22 ^{o}C), $t_{1/2}$ = 10 hours for **(33b)**, whereas for **(33a)**, the half-life is 1.9 minutes, a reaction rate 300 times faster than that of **(33b)**. At pD 7.0, the rate difference is even faster, with **(33a)** having a $t_{1/2}$ = 5.4 min, while for **(33b)** $t_{1/2}$ = 270 hours, a 3000 fold reactivity difference.

Also investigated was the effect of substitution at one of the carboxylic acid groups for comparison with the study previously illustrated. This involved converting the carboxylic acid group to a methyl ester group (**Figure 1-15**).

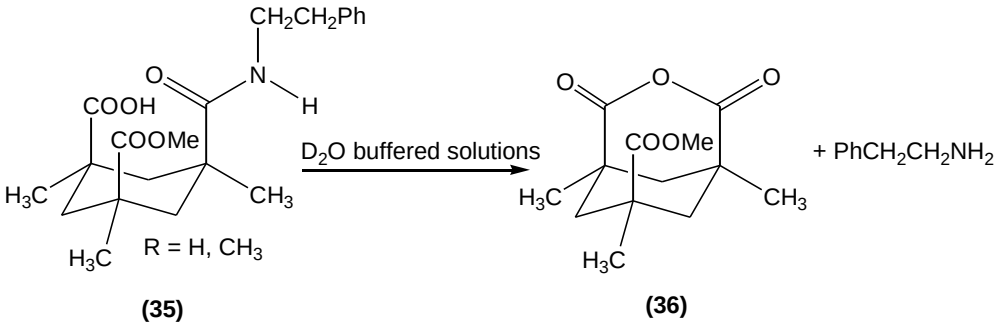

Figure 1-15: Amide acid methyl ester compound studied by Curran *et al*[43]

The full pH-rate profile (pD 0 – 8) for the methyl ester **(35)** showed roughly the same reaction rates as the original secondary amide **(33b)**, so substitution has a negligible effect on the rate of reaction, confirming the experiments conducted by Menger and Ladika. The tertiary analogue of **(35)** could not be isolated for a similar study due to its high reactivity.

It was also found that the *cis,cis* ester **(33b)** exhibits a 100 fold faster rate between pH 5 and 6.3 than the *cis,trans* isomer (**Figure 1-16**). The pH rate profiles for **(37a)** and **(37b)** were plotted, and showed that the *cis,trans* tertiary amide underwent acylolysis up to 100 times faster than the secondary amide.

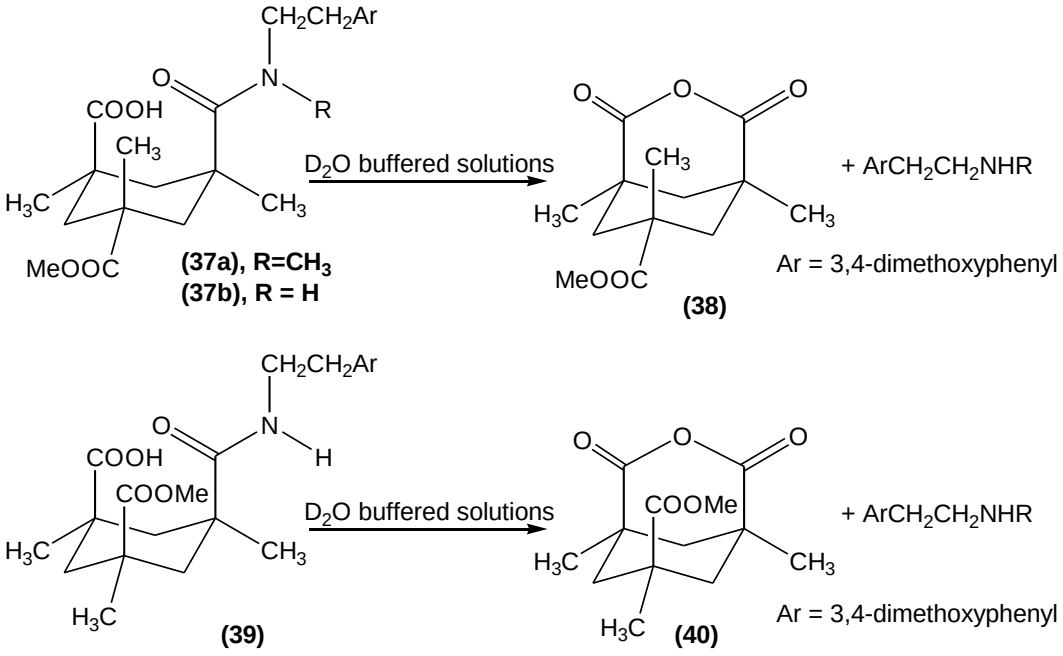

Figure 1-16: *cis,cis* secondary amide and *cis,trans* tertiary and secondary amides studied by Curran *et al*[43]

The rates showed greater differences than expected if, as Menger and Ladika stated, only the proximity of carboxylic acid groups and some 1,3-diaxial strain was postulated as responsible for the amount of intramolecular catalysis observed. Examination of space-filling models for **(33a)**, **(33b)**, **(37a)** and **(37b)** revealed the presence of so-called pseudoallylic strain associated with the amide, arising from interaction between the *N*-substituents *trans* to the C=O bond and the alkyl substituents on the tertiary cyclohexane carbon α to the amide. For the tertiary amide these interactions may be large enough to cause distortion of the amide bond, which is known to accelerate amide hydrolysis.[44] This is proposed as the main cause of rate acceleration for tertiary amides, causing up to 10^5 times rate acceleration where it is present. A study by Dougan *et al*[45] found the same pseudoallylic strain to contribute to the reactivity of their piperidyl Kemp's acid derivative, though they could not quantify accurately the amount of strain relief. Another study conducted in 2006 by Gershler *et al*[46] disputed the large value stated by Curran *et al*[43] estimating that pseudoallylic strain relief contributes only a 2400 fold rate increase in amide bond cleavage.

1.5.2 Doxorubicin system

Doxorubicin is marketed under the name Adriamycin and is a chemotherapy drug used for cancer treatment. Whilst it is effective against a wide range of cancers it is hindered in its effect by its dose-dependent toxicity, especially its cardiotoxicity.[47] In an effort to try and improve its

effectiveness, a study was conducted by Dubowchik *et al*[48] on attaching doxorubicin to an amide of Kemp's acid creating an acid sensitive prodrug. They studied the rate of doxorubicin release at neutral pH (pH 7) versus lysosomal pH (pH ≈ 4.8). Lysosomal pH was used as it was hoped that this type of drug could be targeted at being released inside lysosomes in cells. The molecule would be able to enter the cell via endocytosis using specially created monoclonal antibodies.[49]

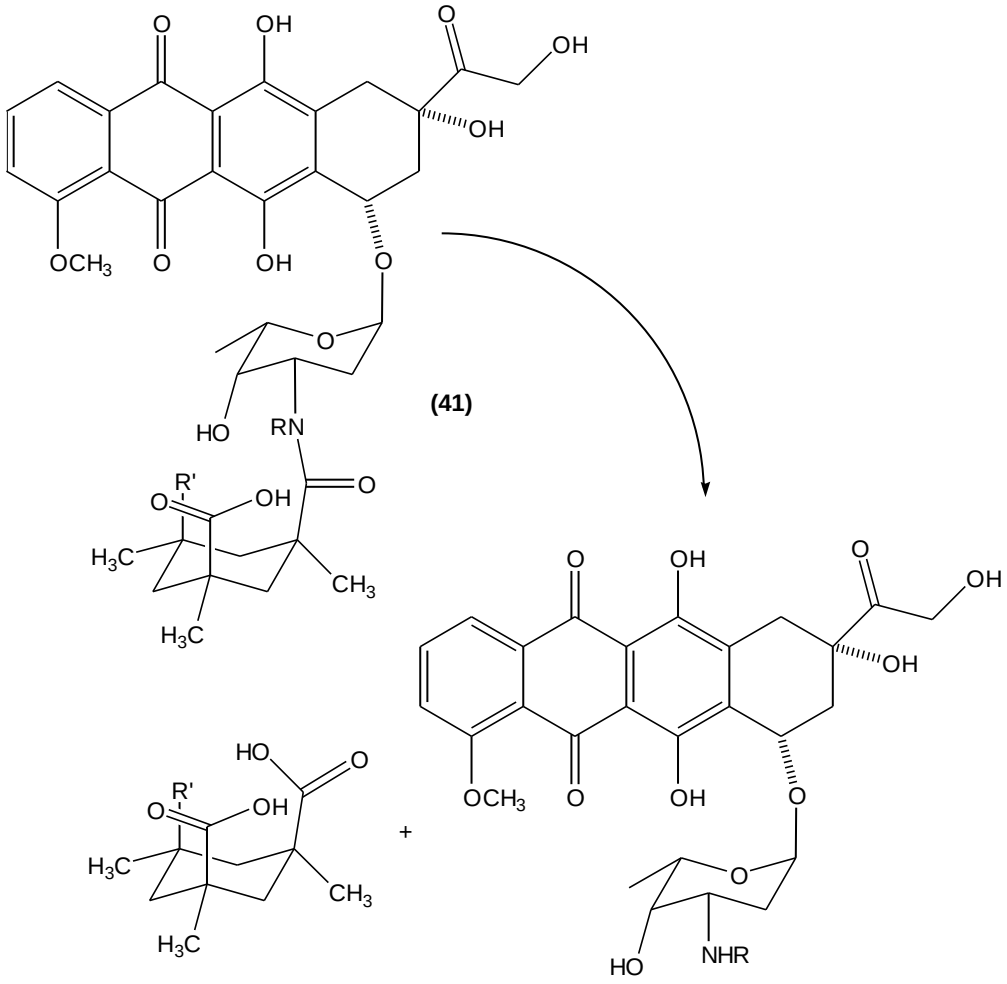

Figure 1-17: Doxorubicin-Kemp's acid/ Kemp's acid amide conjugate[48]

Table 1-3: Effect of various R groups on the rate of doxorubicin release[48]

Compound	**(41a)**	**(41b)**	**(41c)**	**(41d)**
R	H	H	$COCF_3$	H
R’	COOH	CONHBu	CONMeBu	COOMe
$t_{1/2}$, pH 5, 37 ^{o}C	30h	90h	>174h	40h
$t_{1/2}$, pH 7, 37 ^{o}C	--	>160 days	> 174h	>100 days

The doxorubicin molecule was attached as an amide to one of the carboxyl groups (**Figure 1-17**), and in three of the derivatives a second acid group was converted to another amide or to an ester (**Table 1-3**). A second amide or ester group was placed at the R’ position to see what effect it would have on the overall rate of the hydrolysis reaction. Compound **(41d)** with amide and methyl ester groups was found to have the best combination of reaction rates for the hydrolysis leading to doxorubicin release, being extremely unreactive at neutral pH whilst having a half-life of forty hours at pH 5. Thus molecule **(41d)** shows great potential for not only prodrug application, but the use of Kemp’s acid amides as acid-sensitive linkers in prodrug use. However no further studies on this molecular system have been published; it seems that further work that has been done with doxorubicin is to do with linkages to molecular polymers, the study of which is outside the realms of this thesis.

1.5.3 Planned research work

The research work planned for this thesis was the attempted syntheses and characterisation of a *cis,cis* Kemp's acid aryl mono amide and its consequent kinetic study for construction of a pH rate profile. To our knowledge, no kinetic study of hydrolysis of any aryl amides of Kemp's acid has been reported.

An aryl amide was chosen also over an alkyl amide, as being more applicable from a prodrug point of view as aryl amine cytotoxin groups exist that could be attached to the Kemp's acid molecule to form a prodrug for accelerated cytotoxin release into low pH tissue. The absolute rates for an aryl amide of Kemp's acid relative to an aliphatic amide are unknown. However studies with amides of maleic acid[50] show the secondary aryl anilide to be four to five times more reactive than the secondary aliphatic methylamide but 10 times less reactive than the tertiary aliphatic dimethylamide.

Mechanistic differences exist between neighbouring-carboxyl-catalysed hydrolysis of aliphatic and aryl amides[51] but the initial expectation might be from the above that a secondary aryl amide of Kemp's acid would be perhaps 10 times less reactive than the tertiary amides previously studied.[41, 43] However in the work done by Curran *et al*[43], his secondary aliphatic Kemp's amides were about 1000 times less reactive than the *N*-methyl tertiary analogues but this was accounted for by a special pseudoallylic strain effect proposed to distort the amide bond in the tertiary

case. This leaves the Kemp's tertiary amide system as a special case, but for secondary amides the data from Aldersley *et al*[50] could be used to predict that a Kemp's secondary aryl amide might be perhaps four to five times more reactive than the Curran secondary aliphatic amides. This looks to be rather slow for prodrug application, but that ignores the essential differences that the Kemp's scaffold might provide relative to the maleic system studied by Aldersley *et al.*[50]

For this study both tertiary and secondary aryl amides were contemplated. The hydrolysis of the aryl amide is also a relatively simple reaction to monitor as the *N*-aryl group in the molecule is UV-absorbing but much less than the corresponding aryl amide, so that the hydrolysis of the aryl amide group will result in strong UV changes, which allow spectrophotometric monitoring. By comparison with NMR monitoring, UV has the advantage that much more dilute samples in fully buffered aqueous solutions can be used and with stringent temperature control in a thermostatted cell block in the spectrophotometer. This method is also far more reliable for data reproducibility than removing samples for chromatographic analysis as carried out by Curran *et al*.[43]

The aim was that once an amide was synthesised, rate studies would be conducted to construct a pH rate-profile, encompassing the three different ionisation states of the triacid amide.

2 Synthesis of an amide of Kemp's acid

2.1 Introduction

As explained in the introduction, Kemp's acid amides show good promise for prodrug application. However, no Kemp's acid amides are readily available from any commercial sources, so must first be synthesised from Kemp's triacid. This synthesis can be divided into two parts; first the synthesis of the Kemp's anhydride acid chloride and then secondly the use of the anhydride acid chloride to synthesise the desired amide.

As the following discussion shows, initial attempts at directly synthesising a tertiary aryl amide using *N*-methylaniline were unsuccessful. To obtain a secondary aryl amide, the way around difficulties with the direct route from acid chloride was to first synthesize and purify an imide of Kemp's acid, from which the imide ring functionality could be opened in hydroxide solution to yield the secondary amide as the stable dianion, in which state it could be stored in aqueous alkaline solution until required for kinetic study at low pH (**Figure 2-1**).

The intention after successful synthesis was to determine a full pH-rate profile in the pH 4 – 8 region for the diacid amide so that contributions from the three different ionised species (the neutral, mono-ionised and di-ionised species) could be established, something which had eluded earlier studies with Kemp's aliphatic amides. Because the secondary amide could

allow reversion to imide to occur in competition with hydrolysis, checks to determine if this occurred were also planned for. In previous studies this was not an issue because the amides were tertiary.

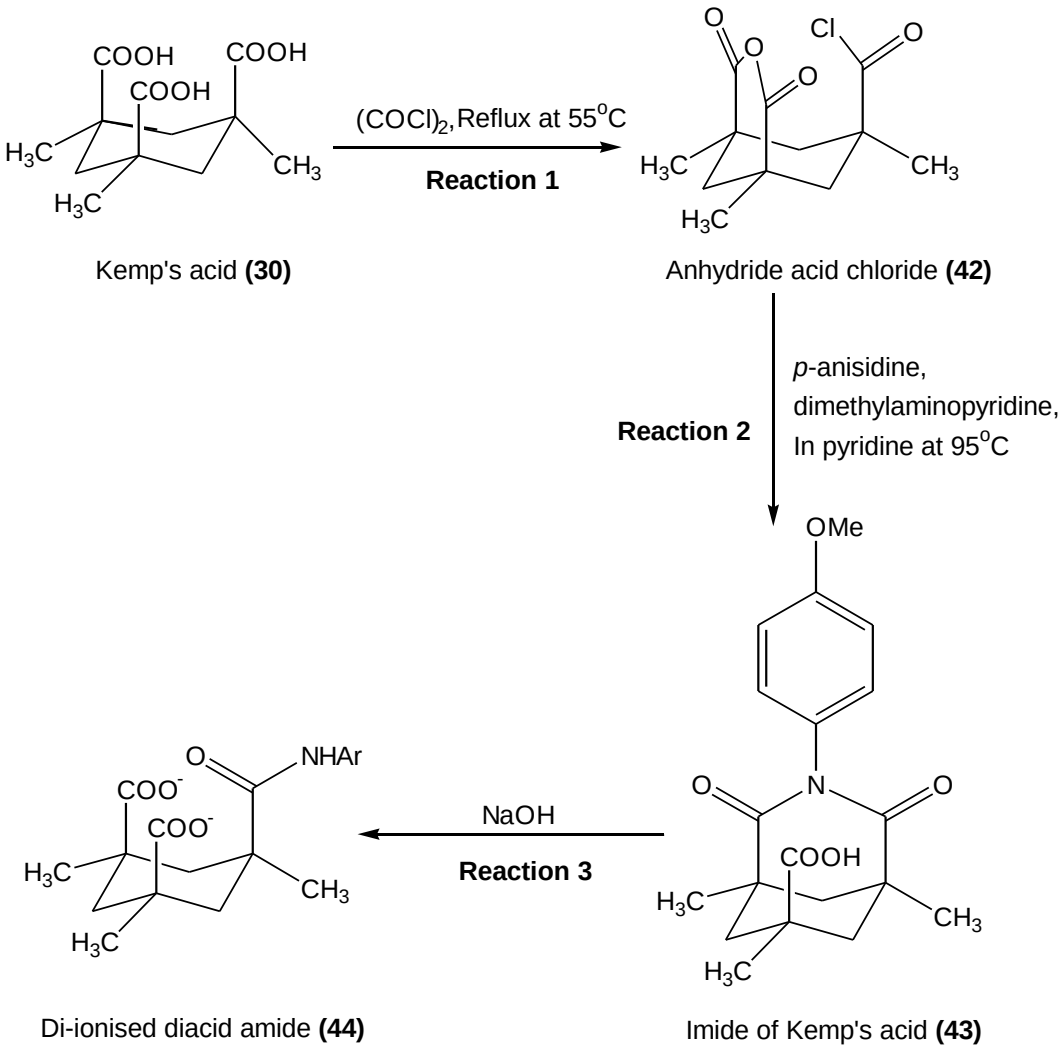

Figure 2-1: Overall synthesis method from Kemp's triacid through to the diacid amide

2.2 Preparation of Kemp's anhydride acid chloride

Kemp reported a method for synthesis for anhydride acid chloride[38] using excess thionyl chloride ($SOCl_2$) under reflux for four hours, after which excess reagent and solvent were evaporated off and then the resultant

product crystallised from toluene. This in principle could have given a tri-acid chloride; however, the anhydride acid chloride was formed suggesting that it may proceed through the mechanism in **Figure 2-2**:

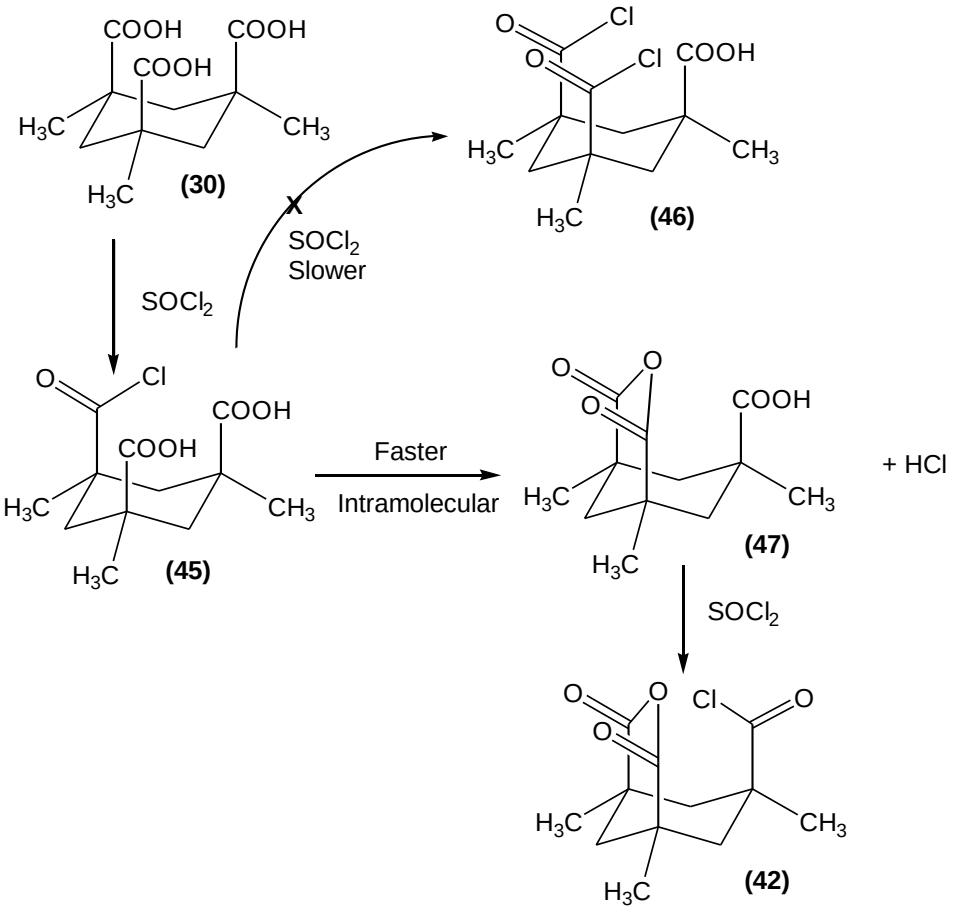

Figure 2-2: Formation of anhydride acid chloride using thionyl chloride

In the current study this method was adopted but instead of $SOCl_2$, oxalyl chloride $(COCl)_2$ was used, which leaves less residue after the excess reagent is removed. Checks to ensure the reagent change did not produce tri-acid chloride were made by IR spectroscopy. There are three previous reports of IR data for the acid anhydride which were used for reference frequencies. Menger and Ladika[41] reported 1793 cm^{-1} and 1770cm^{-1} for

the anhydride and acid chloride groups of their anhydride acid chloride. Ikeura and colleagues[52] reported a single absorbance at 1773cm^{-1} but may have ignored a weak absorbance around 1790cm^{-1}. In Kemp's initial study, he reported a wavelength of 1780cm^{-1}. The discrepancy in wavelengths may come from variation in IR resolution. Reported melting points were in the range of 255-260^{o}C. These two methods of initial monitoring were useful checks prior to structural confirmation by NMR spectroscopy.

The anhydride acid chloride is water sensitive, and any water present during the reaction or on workup will cause hydrolysis with loss of acid chloride if not anhydride. All glassware was dried in an oven in advance and the reaction vessel was fitted with a calcium chloride drying tube. Dry dichloromethane was used as the solvent, as the triacid in insoluble in this medium due to its (three) acid groups, but the product of the reaction, the anhydride acid chloride is soluble, so this provides a handy measure for assessing the completion of the reaction.

2.2.1 Results

This reaction yielded crude white crystals that were initially analysed by melting point and IR spectroscopy. The melting point range of the impure crystals was 245 -248^{o}C, slightly lower than literature values. IR analysis in the carboxyl region further confirmed that the desired product had been formed along with some impurities, showing the expected peaks at 1770 and 1802cm^{-1} with another peak at 1746cm^{-1} all within the range predicted

from earlier studies. A peak was also present at 1850cm^{-1}, which can be attributed to $(COCl)_2$, however using IR to determine if any $(COCl)_2$ was present was difficult as $(COCl)_2$ gives two peaks at 1781 an 1850cm^{-1} that may overlap with those of the anhydride acid chloride. Overall, these initial methods showed that anhydride acid chloride had been formed but there were impurities present, so a recrystallisation with dichloromethane was undertaken. Fine white crystals were obtained which were analysed by NMR, which showed peaks that matched those from the literature[53] and no evident impurities, thus providing final confirmation that pure anhydride acid chloride product sufficiently pure for the next stage had been formed. Another melting point was taken, showing an improved melting point of 253 – 255^{o}C, closely matching those reported by the literature[54].

2.3 Attempted synthesis of a tertiary aryl amide

2.3.1 N-Methylaniline method

Tertiary aliphatic amides of Kemp's acid show much greater reactivity than secondary amides, so the synthesis of a tertiary aryl amide of Kemp's acid was the next logical step for this study.

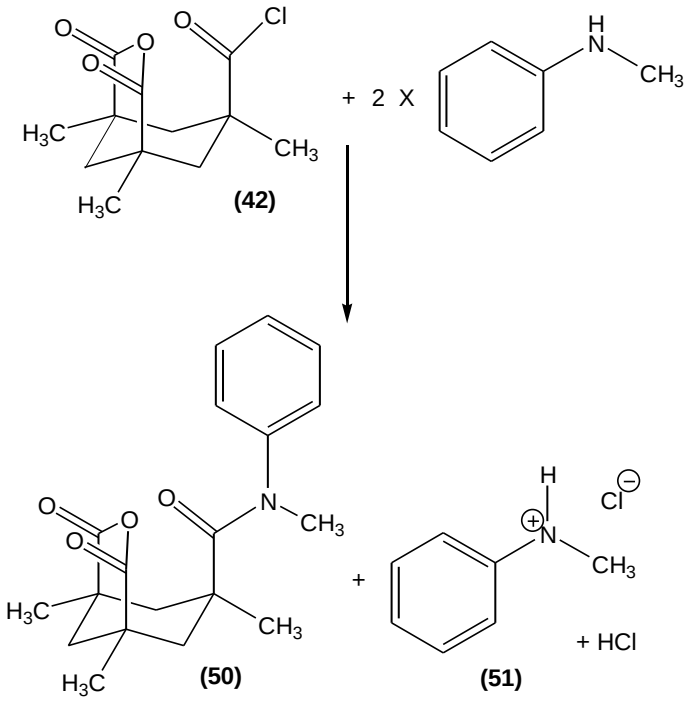

Figure 2-3: Synthesis of a tertiary Kemp's amide using N-methylaniline

Synthetic methods for tertiary aliphatic amides have varied. Curran and colleagues used a combination of *N*-methylphenethylamine and triethylamine in dichloromethane in the synthesis of their variety of tertiary alkyl amides.[43] From the anhydride acid chloride, Menger and Ladika[41] used dry pyridine and pyrrolidine to synthesise tertiary pyrrolidine acid amides. In each case a base was present in excess to remove hydrochloric acid produced. For this study, it was decided that *N*-methylaniline should be used (**Figure 2-3**). During this reaction, one mole of hydrochloric acid (HCl) is formed, which will react with *N*-methylaniline to form the salt **(51)** if there is no other base present, so two moles of the amine *N*-methylaniline are needed, to ensure a complete reaction. The

downside of this is that any product formed **(50)** will be contaminated with the amine salt **(51)**.

The preliminary study of the reaction was carried out in deuterated chloroform in an NMR tube so that the reaction could be monitored by ^{1}H NMR. The absence of any *N*-methylaniline amide signals around 7.4 and 7.1 ppm[54] showed no reaction at room temperature after two hours. Triethylamine, as used by Curran *et al*[43], was then added to potentially promote the reaction through base catalysis of the nucleophilic attack of *N*-methylaniline on the anhydride acid chloride. The solution was heated under reflux for two days, and still no reaction was found to have occurred. The lack of reaction is consistent with much reduced basicity and nucleophilicity if aryl amines relative to aliphatic amines.

2.3.2 Use of butyllithium to generate a more reactive amide ion

It was decided to utilise butyllithium (BuLi) **(52)** to deprotonate the *N*-methylaniline (**Figure 2-4**), and increase its nucleophilic reactivity prior to its reaction with the anhydrous acid chloride. Both reactions needed to be free of water vapour so that BuLi and the anhydride acid chloride do not hydrolyse. All glassware was dried prior to use and fitted with drying tubes, and both reactions were conducted under nitrogen. This reaction was conducted at low temperature (-40 ^{o}C) on a 1,2-dichlorobenzene slush bath in an attempt to maximise selectivity of *N*-methylaniline for acid chloride over less reactive anhydride. For the first attempt, dry dichloromethane was used as the solvent in both stages, but the reaction

to form the tertiary amide did not occur in this medium. The possibility of a side reaction of the amide as base on dichloromethane to form a chlorocarbene could not be excluded, so both steps were again attempted with sodium-dried diethyl ether solvent.

2.3.2.1 Deprotonation reaction

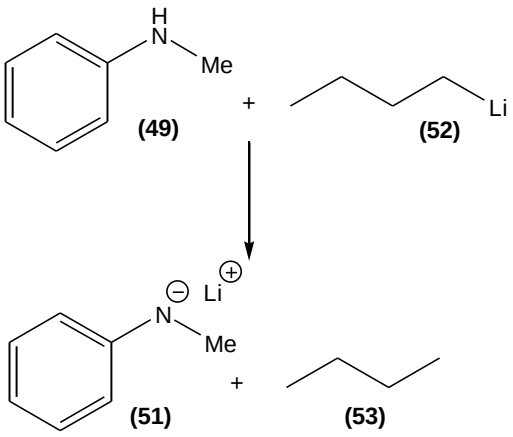

Figure 2-4: Deprotonation of N-methylaniline **(49)** by n-BuLi **(52)**

The N-methylaniline was dissolved in the dry solvent in the reaction vessel and n-BuLi solution (in cyclopentane) in dry diethyl ether solvent was injected into this solution dropwise with stirring. This resulting pale yellow solution was placed in the refrigerator overnight in preparation for the next phase of the reaction.

2.3.2.2 Reaction of deprotonated N-methylaniline with anhydride acid chloride

This step of the reaction was also conducted on a low temperature slush bath, so that the desired anhydride amide product **(54)** did not react with **(51)** again to form any acid diamde **(55) (Figure 2-5)**. For the first attempt

at this reaction, the anhydride acid chloride was dissolved in the dry dichloromethane, and the lithium amide **(51)** added slowly (1.3 x excess to allow a margin for trace water contamination).

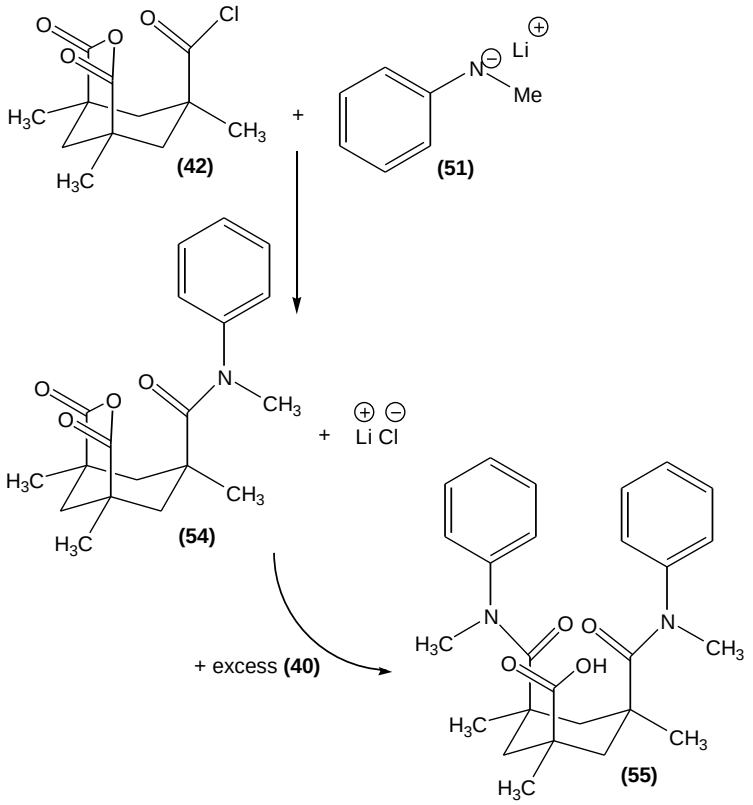

Figure 2-5: Formation of tertiary amide from deprotonated N-methylaniline

Addition of all the deprotonated amine caused the solution to turn a dark brown colour. Upon completion of the addition, the solution was left to stand overnight at room temperature. Some brown crystals had settled out of the solution. The supernatant was removed and analysed as a solution spectrum by IR. The spectrum showed no expected amide peaks and peaks were seen that matched the initial anhydride acid chloride peaks. NMR analysis was also conducted in a last attempt to see if any product **(54)** had been formed. The peaks observed were characteristic of an

amine, and there was no sign of the *N*-methylaniline signal of an amide. The brown crystals were washed with dry dichloromethane and then distilled water. An IR spectrum of these crystals also showed no amide peaks as compared to literature values[37, 41] which are in the range of 1600-1630cm^{-1}.

When the NMR solution was left to stand overnight, a white suspended solid had formed on top of the solvent surface, possibly some unreacted Kemp's acid or a salt such as lithium chloride (Li^+Cl^-).

2.3.3 Imide synthesis

After the previous failings of trying to synthesise a tertiary amide derivative of Kemp's acid directly, it was decided to first synthesise an imide to act as an "intermediate" that could then undergo a ring opening reaction to form an acid amide. In this case however, it would be a secondary amide (**Figure 2-6**), so a subsequent test to ensure the amide did undergo hydrolysis rather than reform imide around neutral pH would be needed. This method has been used by Rebek *et al* [39] who reacted the anhydride acid chloride with a one molar equivalent of aniline and a catalytic amount of dimethylaminopyridine (DMAP) in pyridine.

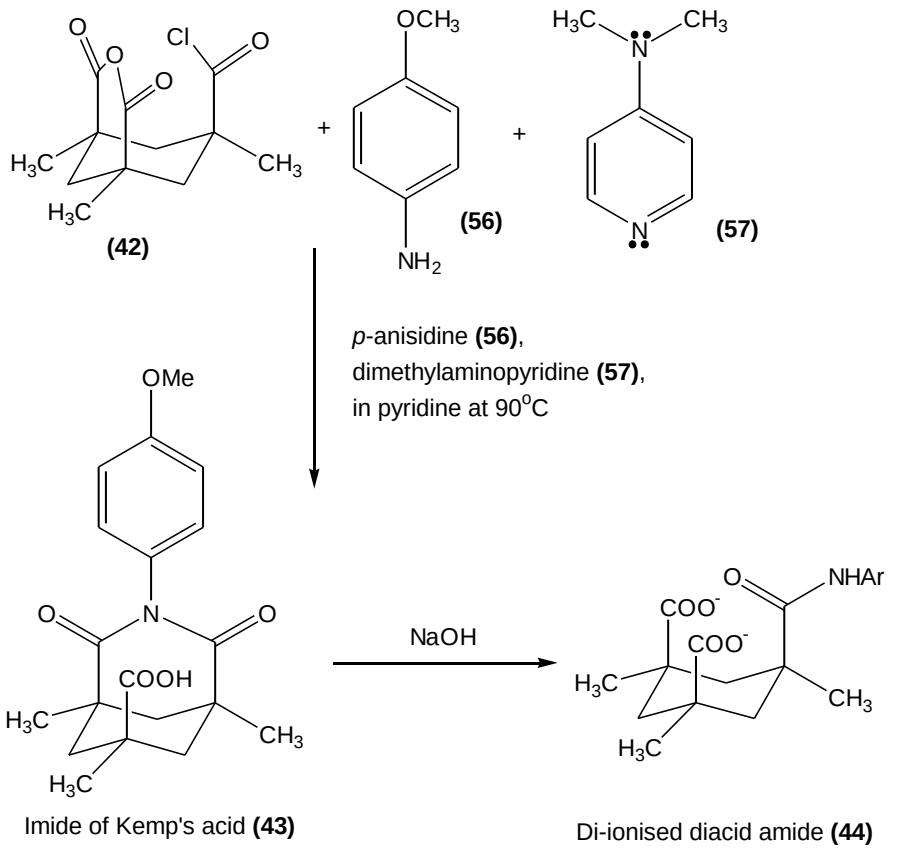

Figure 2-6: Synthesis of an amide of Kemp's acid via an imide and subsequent ring opening to form a diacid secondary amide

This imide could then serve as the reactant for a ring opening reaction, in NaOH in which the imide hydrolyses to yield a diacid amide (**(44)** in **Figure 2-6**) which is a stable form of the substrate needed for hydrolysis study at lower pH.

The imide **(43)** was successfully prepared using *p*-anisidine as described in the experimental section after a prolonged reaction under nitrogen at 95 ^{o}C for a week.

2.4 Experimental

^{1}H NMR spectra were collected at either 300 MHz on a Bruker Avance 300 FT-NMR or at 400 MHz on a Bruker Avance DRX400 FT-NMR spectrometer. Infra-red spectra were recorded either as a solid disc with KBr or as liquid solution spectra between KBr discs on a Perkin-Elmer spectrum 100 FT-IR spectrometer. Melting points were obtained on a Reichart-Jung Thermavar microscope thermometer. Elemental analysis was carried out by the Microanalytical laboratory at Otago University.

2.4.1 Anhydride acid chloride (42)

Kemp's triacid (0.5 g, 1.95 mmol) was dissolved in dry dichloromethane (20 mL) as solvent. A five times excess of oxalyl chloride was added dropwise (1.68 mL, 9.75 mmol). This reaction solution was heated under reflux on an oil bath set at 55 ^{o}C until all of the Kemp's triacid had disappeared, indicating the completion of the reaction of Kemp's triacid to the soluble anhydride acid chloride. The resulting solution was left to cool overnight. Some crystallisation occurred and the remaining solvent was removed by rotary evaporation. This yielded crude white crystals. Purification was achieved by dissolving the crude product in dry dichloromethane (10 mL), again refluxing until all of the crude crystals dissolved. Excess solvent was again removed by rotary evaporation and then on a vacuum line. The anhydride acid chloride was isolated as fine white crystals (0.253 g. 50%, m.p. 253 - 255 ^{o}C). ^{1}H NMR (300 MHz)

($CDCl_3$) (numbering scheme illustrated in **Figure 2-7**): δ 1.25 (*d*, J = 14.37 Hz, 2H, axial H2, H6), 1.32 (*s*, 3H, H1'), 1.34 (*s*, 6H, H3', H5'), 1.37(*d*, J = 14.91Hz, 1H, axial H4), 2.02 (*d*, J = 1.83 Hz, 1H, equatorial H4), 2.74 (*d*, J = 13.76 Hz, 2H, equatorial H2, H6). IR (liquid solution in CH_2Cl_2): 1746 (anhydride C=O), 1770 (anhydride C=O), 1802 cm^{-1} (acid chloride C=O).

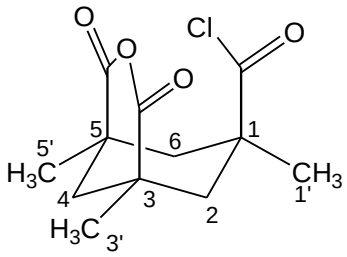

Figure 2-7: Anhydrous acid chloride, numbered for NMR assignments

2.4.2 Attempted tertiary amide acid synthesis using N-methylaniline

The *N*-methylaniline was distilled prior to the reaction, collecting a middle fraction (b.p. 194-196^{o}C). The anhydride acid chloride (48.5 mg, 0.187 mmol) was dissolved in deuterated chloroform (3 mL). A sample of this solution (0.031 mmol) was placed in an NMR tube to which a twofold excess of *N*-methylaniline was added (6.8 µL, 0.062 mmol). After two hours the solution was analysed by NMR which showed the methyl signal of amine but not of amide peaks around 7.4 and 7.1 ppm[54], indicating that no reaction had occurred. Triethylamine was therefore added in a 1.5 fold excess relative to *N*-methylaniline (13.1 µL, 0.94 mmol). This solution was heated under reflux in a nitrogen atmosphere for two days and then re-analysed by NMR spectroscopy. This showed strong signals from

triethylamine and also *N*-methylaniline but once again not the desired methyl amide peak.

2.4.3 Attempted tertiary amide acid synthesis using deprotonated N-methylaniline

N-Methylaniline (165 µL, 1.52 mmol) was placed in diethyl ether (AnalaR, 6 mL) which had been dried over a weekend with sodium wire. n-Butyllithium in cyclopentane solution (0.76 mL, 1.52 mmol) was added slowly to the ether solution, cooled in a 1,2-dichlorobenzene slush bath at -40 ^{o}C.

Kemp's anhydride acid chloride (0.253 g, 1.17 mmol) was dissolved in dry diethyl ether (30 mL) and cooled to -40 ^{o}C in a dichlorobenzene slush bath. The lithium amide **(51)** solution (6 mL) was added dropwise via syringe to the anhydride acid chloride solution. This was reacted on for two hours with a drying tube fitted to the reaction solution. After leaving to stand overnight, crystals had formed in the solution along with supernatant. The supernatant was removed and initial analysis was achieved by IR, which showed no amide carbonyl peaks. An NMR spectrum was taken which showed peaks representative of the *N*-methylaniline and Kemp's anhydride acid chloride, showing no signs that an amide had formed.

The separated crystals were taken and then washed in a separating funnel with dry diethyl ether (40 mL) and then distilled water (20 mL). These

cleaned crystals were then dissolved in $CDCl_3$ and analysed by IR, once again showing no amide peaks.

2.4.4 Synthesis of an Imide of Kemp's acid (43)

Pyridine (AnalaR) was distilled over KOH and dried with oven-dried 3A type molecular sieves. *p*-Anisidine was doubly recrystallised from ethanol, and vacuum dried. The anhydride acid chloride was dissolved in pyridine (5 mL), to which p-anisidine (1.2 mol equivalent, 0.298 g), and a catalytic amount of dimethylaminopyridine (0.03 g) was added. The solution was heated at 95 ^{o}C for seven days under nitrogen.

A 1 mL sub-sample was taken and extracted by the scheme outlined below, which was adapted from a similar extraction method used by Rebek *et al*[39]. This method of extraction yielded brown crystals. These crystals were then analysed by IR and ^{1}H NMR spectra (in $CDCl_3$). The NMR spectrum of the sample showed that the imide product had been formed along with some impurities. After the initial NMR, a white solid had formed on top of the $CDCl_3$ solution. The solid was removed and analysed by IR and melting point analysis and was found to be Kemp's acid, showing that in the reaction mix some of the original material had been reformed presumably by hydrolysis of acid chloride.

The remainder of the reaction solution was then extracted. The extracted solution had excess solvent removed by rotary evaporation which yielded light brown crystals which were analysed by NMR. The spectrum showed that this product was much cleaner than the sub-sample analysed

previously, and contained only the desired imide product, as assessed by comparison[39] with reported the spectrum for a close analogue with a butyl group in place of methoxy on the aromatic ring. The ring opening reaction will be covered in the next chapter, as it falls under kinetic analysis.

Recrystallisation was carried out in ethanol (AnalaR) and then letting the pure crystals isolate out of solution.

The extraction method that was used is outlined here (with its rationale):

Step 1: The sample was extracted with sodium bicarbonate, which ionises the COOH group on the imide so that it dissolves in the aqueous medium.

$RCOOH + HCO_3^- \longrightarrow RCOO^- + H_2O + CO_2$

$RCOO^-$ is water miscible, but pyridine and dimethylaminopyridine may also dissolve, however there was no insoluble material present after this step of the extraction.

Step 2: The aqueous bicarbonate extract was acidified with 2 mol L^{-1} hydrochloric acid to pH 2. This neutralises the acid but ionises all the pyridine and aromatic amine (**Figure 2-8**)

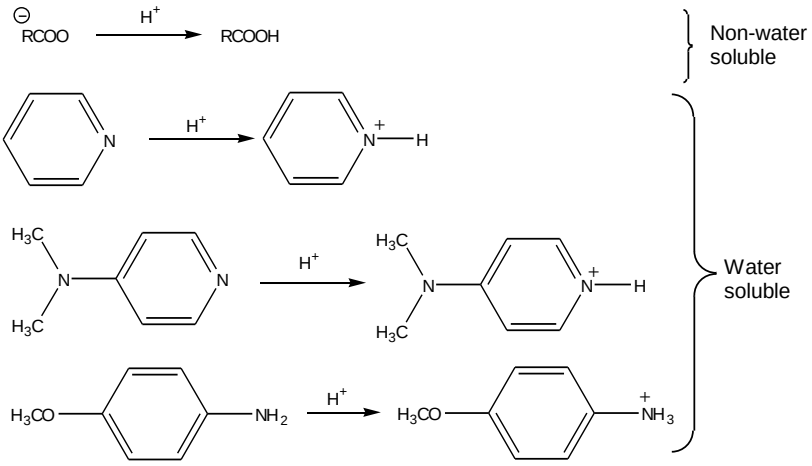

Figure 2-8: Ionisation of acid and aromatic amine groups in step 2 of extraction

Step 3: Two extractions were done with dry dichloromethane (20 mL) in a separating funnel. The desired acid imide product can be extracted into dichloromethane (as it is not water soluble) and leave the other ionised compounds in the water layer.

Step 4: The two organic fractions were combined and washed with distilled water (10mL) to remove any inorganic residues. The combined fractions were then dried with granular $CaCl_2$ and filtered.

Step 5: Removal of dichloromethane under vacuum.

This yielded light brown crystals (0.201g, 29%, m.p. 259 – 262 ^{o}C) of **(43)**; found: C, 66.02; H, 6.71; N, 4.01; calculated for $C_{19}H_{23}O_5N$: C, 66.07; H, 6.71; N, 4.06 %. ^{1}H NMR (300MHz) (CDCl3) (numbering scheme illustrated in **Figure 2-9**): δ 1.27 (d, J = 14.73 Hz, 2H, axial H2 and H6), 1.32 (s, 3H, H3'), 1.47 (d, J = 12.87 Hz, 1H, axial H4), 2.12 (d, J = 13.57 Hz, 1H, equatorial H4), 2.16 (s, 6H, H1' and H5'), 2.83 (d, 2H, equatorial H2 and H6), 3.78 (s, 3H, H10'), 6.88 (d, J = 9.18 Hz, 2H, H8), 7.00 (d, J = 8.52 Hz, 2H, H9). IR (CH_2Cl_2): 1687 (imide C=O), 1734cm^{-1} (carbonyl C=O).

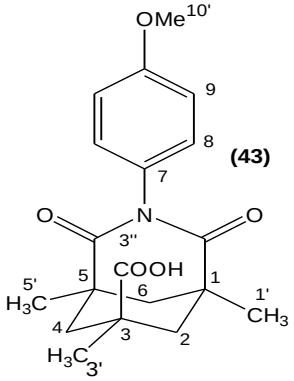

Figure 2-9: Imide of Kemp's acid, numbered for NMR assignments

3 Kinetic studies

3.1 Introduction

Kinetic work was started with the overall goal of seeing whether the synthesised amide diacid **(44)** would undergo the desired hydrolysis reaction to release amine or whether it would reform imide, a reaction which releases no amine and therefore has no prodrug application (**Figure 3-1**). This was of concern because similar studies by Billett *et al*[37] on cyclopentane aryl amide triacid systems (**section 1.4.10**) showed that just below neutral pH, hydrolysis was minor whereas imide formation was the major reaction. The aim was that if hydrolysis was determined to be at least the main reaction then the study could be extended further to try and determine a pH rate profile across the acid ionisation range for the hydrolysis reaction. **Figure 3-2** shows an idealised picture of such a rate profile assuming the diacid to be hydrolytically more reactive than the mono-acid. The focus would be on the pH range of 5.8 – 7.3 as this is the region of main interest with respect to prodrug activity, but establishing individual rate constants for the neutral and mono-ionised diacid amides if their hydrolysis rates are sufficiently different to be dissectible was also of key interest for reactivity analysis. In Menger and Ladika's[41] study with their tertiary aliphatic amide such dissection was not possible suggesting very similar rates for the mono- and diacid species.

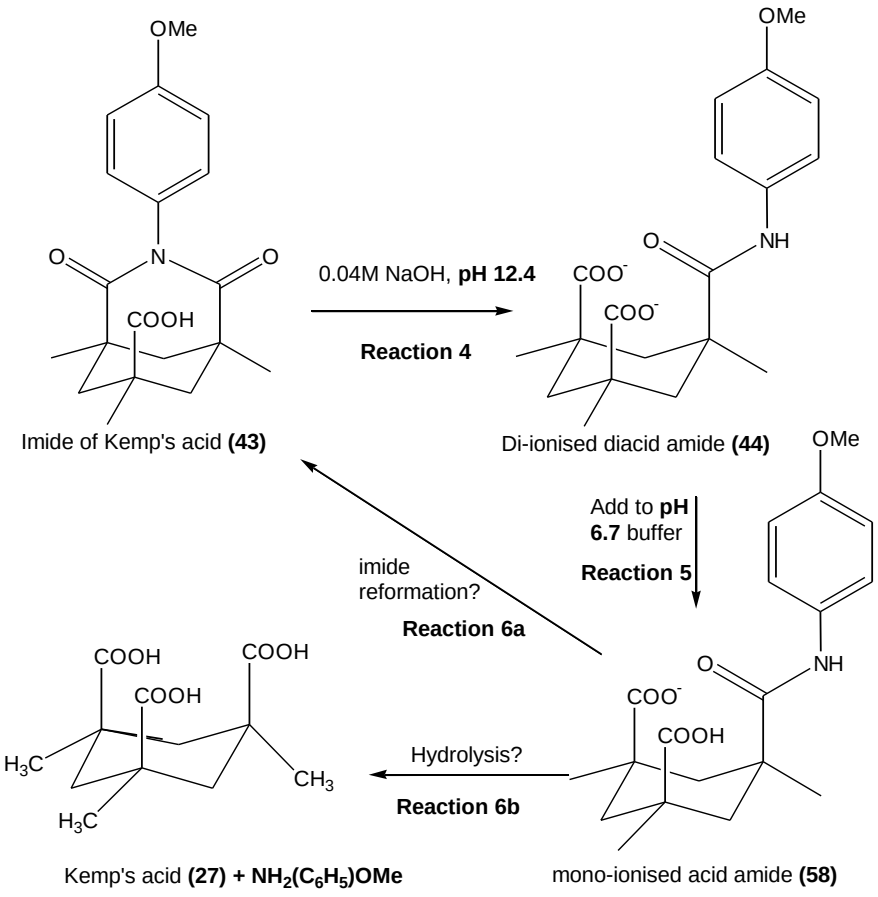

Figure 3-1: Summary of the reactions studied by kinetic analysis

3.2 Initial repetitive scanning

These initial scanning studies were initiated with the ultimate goal of seeing whether the Kemp's amide **(58)** would hydrolyse to reform the original triacid and release amine and/or reform the imide, but as the imide initially needed to be opened in basic solution to form the amide (in its stable fully ionised state at high pH), this reaction was the one initially studied. Subsequent monitoring of the reaction of the triacid amide after the pH reduction followed. Some initial repetitive scanning reactions were conducted on the impure imide that was first isolated. Further studies

including the rate measurements were then done with the purer imide, all of which are summarised below.

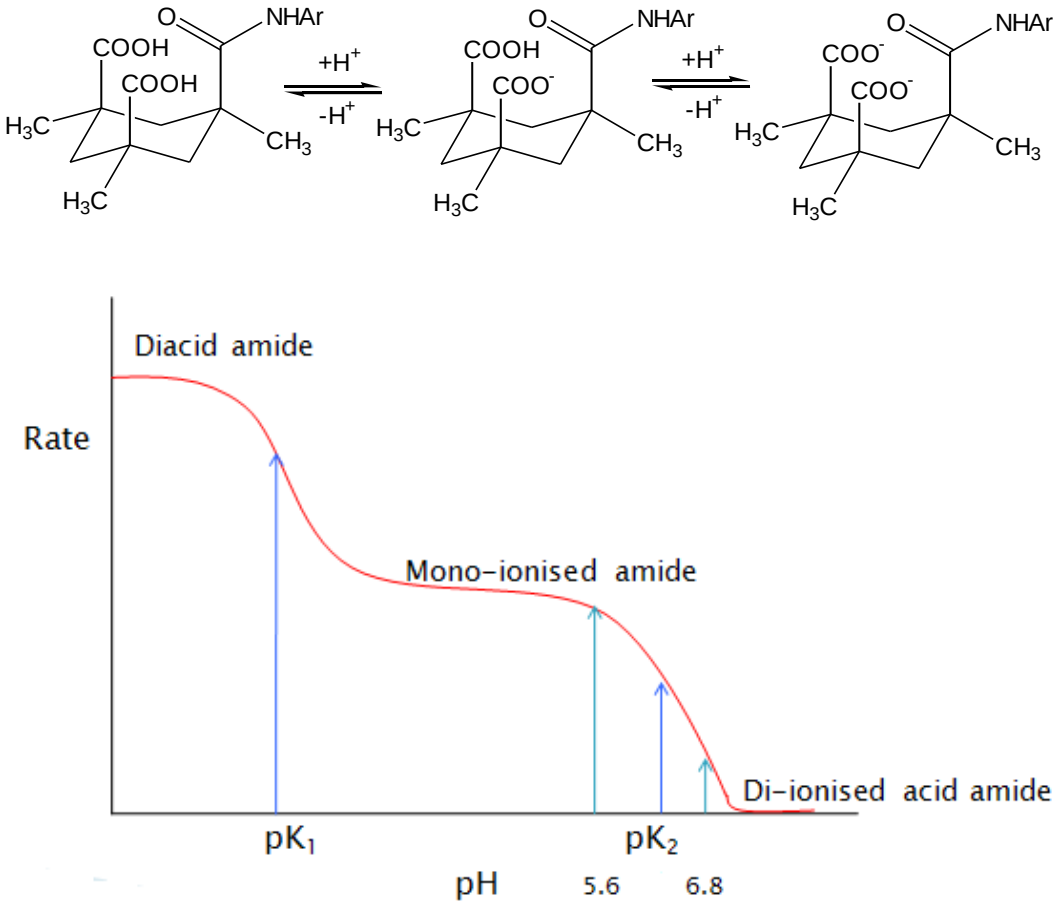

Figure 3-2: Expected pH rate profile for an amide of Kemp's acid

3.2.1 Kinetic studies on the imide ring-opening reaction

The studies conducted on this reaction were done on a Kontron Uvikon 810 spectrophotometer. Initially the ring-opening reaction of the imide was studied in 0.04 mol L^{-1} NaOH, and spectra showed increased absorbance at 245 nm which is indicative of the imide being hydrolysed to form the di-ionised diacid amide **(44)**, but could also additionally represent the amide reacting further to form Kemp's acid **(27)** and $(C_6H_5)NH_2$. The spectra were

recorded over fifty and 100-minute intervals and the last scan collected after a 250 minute period. The reaction appeared from sequential spectra to be a single one from a tight isosbestic point at 233 nm. This suggested that only the ring-opening reaction was occurring and that the diacid amide product **(44)** was stable in the conditions in its fully ionised state, which was confirmed by the following experiments.

3.2.2 Lowering of pH to 6.7

The pH of this solution of ring-opened product was then reduced by addition to a KH_2PO_4 solution to give some neutral solution and buffering. This solution was again monitored by repetitive scanning. There were two aims in this experiment:

(i) If the previous reaction had produced the di-ionised diacid amide **(44)** **(reaction 4, Figure 3-1)** and it was stable at high pH, lowering the pH would lead to the mono-ionised species **(58)** forming, with its hydrolysis reaction **(reaction 6b, Figure 3-1)** (or some other reaction) at pH 6.7 now to be expected by analogy with earlier studies of Kemp's amides; whereas if the di-ionised amide had already hydrolysed further to amine and Kemp's acid at high pH, no further reaction could occur and there would be no spectral changes at the lower pH. The results from these scans showed there were major spectral changes so this was good evidence that they are those of the reaction of the di-ionised amide and that it was the stable product of the single-stage alkaline ring-opening reaction.

(ii) The spectral changes might show whether the amide was reacting to reform the imide **(reaction 6a)** and/or amine and acid by hydrolysis **(reaction 6b)**, the latter as expected from previous studies with Kemp's acid[43, 53] in which the aliphatic amides employed were always tertiary so were unable to form imides.

In the event, there was a reaction with a tight isosbestic point at about 233 nm (which was seemingly coincident with that observed at higher pH for the imide to amide reaction). In some preliminary studies this isosbestic point had been seen to be lost over time and attributed to the possibility of a second reaction. However the change subsequently disappeared when a purer sample of the imide was used to make the stock solution, indicating the initial importance of absolute sample purity for UV studies like these ones.

3.2.3 Raising pH to 12.4 to check for further imide reaction

Initially, as a result of the coincidence of the two isosbestic points, a likely explanation was initial rapid formation of imide, not hydrolysis. However, part of the alkaline diacid amide **(44)** reaction solution used in this pH-lowering study had been kept aside and it was reacted again in KH_2PO_4 solution. At about the time of the halfway point of the initial reaction at pH 6.7 this sample was raised back to pH 12.4 (approximately equivalent to the pH of the 0.04 mol L^{-1} NaOH), with the aim of detecting any reversal of imide formed back to amide, with increasing absorption as in the initial scans referred to above for 0.04 mol L^{-1} NaOH. As it eventuated, no such

reaction was observed which negates the possibility that there was any imide now present, and suggests that if any imide is formed at pH 6.7 from the amide it must be minimal, or otherwise have reacted itself so quickly at this pH that it is not present at the mid-stage of the apparent initial amide reaction. This evidence suggests that the coincidence of the isosbestic points in the two reactions must indeed be a coincidence, that is to say that the actual product of the initial amide reaction, the amide, and the imide must all have very similar absorbance intensity (extinction coefficient) at 233 nm.

A similar test was done on the original reaction solution after reaction to completion at pH 6.7 in which its pH was raised to 12.4 and the solution re-monitored. This also showed the absence of any reaction and therefore the absence of any imide at completion. Later, a sample of imide was dissolved directly into pH 7 buffer solution and there were no absorbance changes over several days; the imide is quite stable at this pH.

These initial studies showed that the desired amide hydrolysis reaction was occurring essentially exclusively as far as could be ascertained at pH 6.7. This is promising from a prodrug perspective as the hydrolysis reaction is the model for prodrug release. The likelihood of anhydride formation as the first step of hydrolysis is of no detriment to the prodrug potential at this stage as the subsequent anhydride hydrolysis reaction would only occur after the cytotoxin release. The analysed amide solution shows the amine at its λ_{max} and the lack of UV evidence of a second

phase means that the anhydride hydrolysis is either occurring fast relative to the amine release or, less likely, that it gives insufficient absorbance change in the UV range being monitored (230 – 300 nm) to influence the retention of a singe sharp isosbestic point.

After this positive confirmation of the hydrolysis of Kemp's diacid amide, the next step was to get an initial idea of the rates of reaction which could then be accurately determined in the construction of a pH-rate profile.

3.3 Initial studies on the rate of the ring-opening reaction (reaction 4)

As a complement to the amide hydrolysis study, the kinetics of imide ring-opening with hydroxide was also studied. This was achieved by monitoring absorbance changes of solutions of imide in KOH solutions (0.02 – 0.1 mol L^{-1}). For second order kinetics (as this reaction is assumed to be), the rate constant equation is:

$$\text{Rate} = k_2 [OH^-] [\text{imide}] \qquad \textbf{(equation 1)}$$

However for each reaction $[OH^-]$ can be considered constant, as it is in large excess over the imide (which may be as low as 10^{-3} mol), so therefore the rate equation becomes pseudo-first order and simplifies to:

$$\text{Rate} = k_{obs} [\text{imide}] \qquad \textbf{(equation 2)}$$

where k_{obs} is the observed pseudo first order rate constant. Thus the ring-opening reaction can be treated as first order as long as there is a large

excess of OH^-. Since $k_{obs} = k_2 [OH^-]$ from above **(equation 2)**, a plot of k_{obs} versus $[OH^-]$ will result in a straight line with slope k_2 and an intercept of zero (**Figure 3-4**), assuming **equation 1** is the correct rate form and there is no term of higher order in $[OH^-]$.

Absorbance data were used to calculate k_{obs} for each run using the infinity plot method, as a constant steady infinity absorbance was always observed. Some checks were made using the Guggenheim method[55, 56], but the experimental error was larger. The latter method may have been more reliable was there any infinity drift, that is to say if amide reacted further to hydrolyse in stronger base, but there was no evidence for such a reaction occurring.

The infinity method involved letting the desired reaction proceed to a time where a large number of half-lives have elapsed and there is no further absorbance change. At this point the reaction is assumed to have gone to completion and the maximum absorbance value has been reached, denoted as the infinity value (A_∞). By then subtracting all other absorbances from A_∞ and taking the $\log_{10}$ of this absorbance difference ($A_\infty - A_t$), a graph of $\log_{10}$ of the absorbance difference can be plotted against time to yield a graph such as the one illustrated below. The slope of this is $k_{obs}/2.303$ from the second order rate constant (a derivation for this slope equation can be found in Jencks[57]).

The studied reaction was monitored at 243 nm as this is the λ_{max} of the product. All plots of log ($A_\infty - A_t$) versus time were found to be linear and

therefore obey first pseudo first order kinetics. An example of such a plot is provided in **Figure 3-3** with example calculations. The vertical lines on the graph represent estimated experimental error in (subtracted) $A_\infty - A_t$ values.

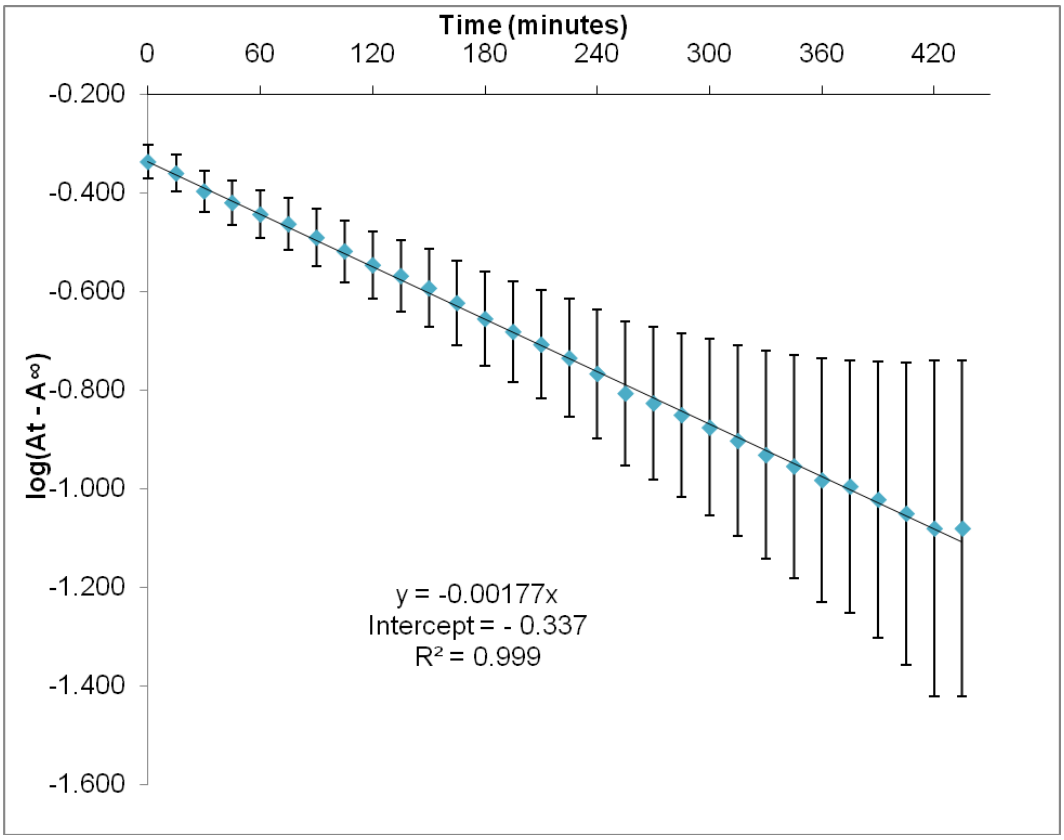

$$k_{obs} = -2.303 \times \text{slope} = -2.303 \times (-0.00177\ \text{min}^{-1}) = 0.00408\ \text{min}^{-1}$$

$$t_{1/2} = \ln(2)/k_{obs} = 170\ \text{min}$$

Figure 3-3: Plot of log ($A_t - A_\infty$) versus time for the ring-opening reaction of **(40)** at 30^0C, 0.100 mol L^{-1} [OH^-] with error bars, assuming a 5% error in absorbance

Table 3-1: k_{obs} (min^{-1}), k_2 (L mol^{-1} min^{-1}), k_2 ($k_2 = k_{obs}$/KOH concentration) and half-lives (min) for different KOH concentrations, with estimated ± 5% error

KOH Concentration (mol L^{-1})	k_{obs} (x 10^{-3}) (min^{-1})	k_{obs} (x 10^{-5}) (s^{-1})	k_2 (x 10^{-4}) (L mol^{-1} s^{-1})	Half-life (min)
0.0200	0.806 ± 0.040	1.34 ± 0.07	6.72 ± 0.34	860
0.0500	2.17 ± 0.11	3.62 ± 0.18	7.23 ± 0.36	320
0.0700	3.01 ± 0.15	5.02 ± 0.25	7.12 ± 0.36	230
0.100	4.08 ± 0.20	6.8 ± 0.34	6.8 ± 0.34	170

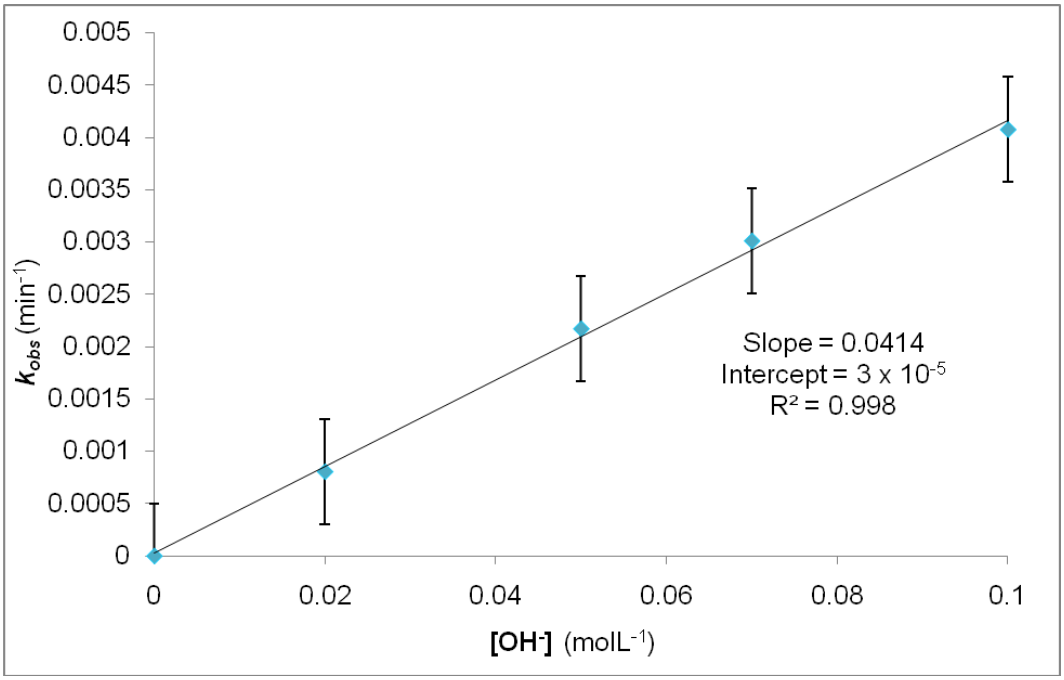

Figure 3-4: Infinity method plot of [OH^-] vs. k_{obs} for hydrolysis reaction with error bars showing 5% error estimate

The calculated half-lives vary with [OH^-] concentration, from 860 minutes at 0.02 mol to 170 minutes at 0.1 mol [OH^-] for the infinity method. The

intercept is at zero, indicating that the reaction follows pseudo first order kinetics and is not subject to complication from any OH-uncatalysed release reaction which has been observed with some imides (as discussed in **section 3.3.1**).

3.3.1 Discussion

From comparison with the imide ring-opening reactions that were observed by Billett and colleagues, he observed much faster rates of reaction for the ring-opening reaction of his imide **(25a, Figure 3-5)** (in its dianionic state), with a k_2 of 0.57 L mol^{-1} s^{-1} under similar conditions (30.1 ^{o}C, μ = 1.0 mol L^{-1}) and half-lives of 5.9, 11.7 and 26.3 s for KOH concentrations of 0.0050, 0.0100 and 0.0200 mol L^{-1}.

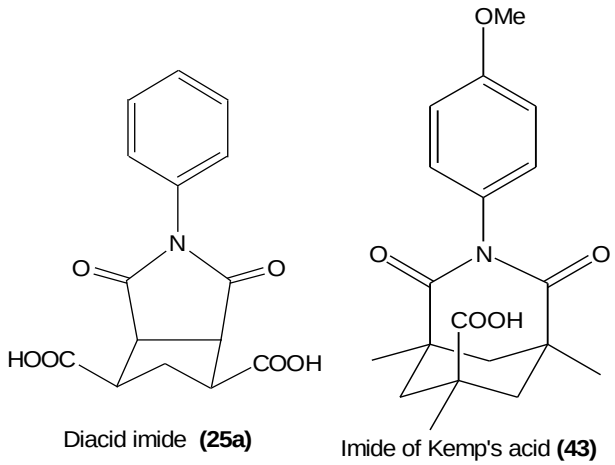

Figure 3-5: Structures of the Billet *et al*[37] imide **(25a)** and the Kemp's acid imide **(43)**

The k_2 of the imide in the current Kemp's case was equal to 0.00067 L mol^{-1} s^{-1}, a reactivity difference of 850 times lower than that found for **(25a)**. For the Billett *et al*[37] compound, the two ionised carboxylic acid groups

should repel the OH^- group that hydrolyses the imide group more than the one ionised group present on the Kemp's mono-ionised acid imide **(43)**. However, the positioning of the COO^- groups to the imide functionality is critical, and the positioning of the carboxylate group in the Kemp's molecule **(43)** would, from the known all-axial arrangement of acid group, be very close to the imide functionality providing more electrostatic repulsion than the two more remote COO^- groups in **(25a)**. The five-membered ring structure for **(25a)** is also less rigid than the Kemp's structure **(43)** so groups have more freedom to allow OH^- less hindered attack.

Studies of imide hydrolysis are scare in the literature. One such study was conducted by Behme and Cordes[58] on the hydrolysis of the imide group of *N*-acetylsalicylamide in alkaline solution (**Figure 3-6**). This gave k_2 equal to 0.0125 L mol^{-1} s^{-1} (25 ^oC), twenty times faster than the hydrolysis rate observed for **25a**. The reaction mechanism illustrated in **Figure 3-6** shows how the imide is hydrolysed reversibly by the OH^- group. At lower concentrations of OH^-, the reaction is first order in $[OH^-]$ and forms salicylamide **(62)** from a di-ionised state **(60)** At higher concentrations of OH^-, the reaction becomes second order and a second equilibrium occurs to form the tri-ionised species **(61)**, from which the product amide **(62)** is still formed, but the formation of this intermediate leads to a loss of linearity between rate and $[OH^-]$ at increasing concentrations of $[OH^-]$..

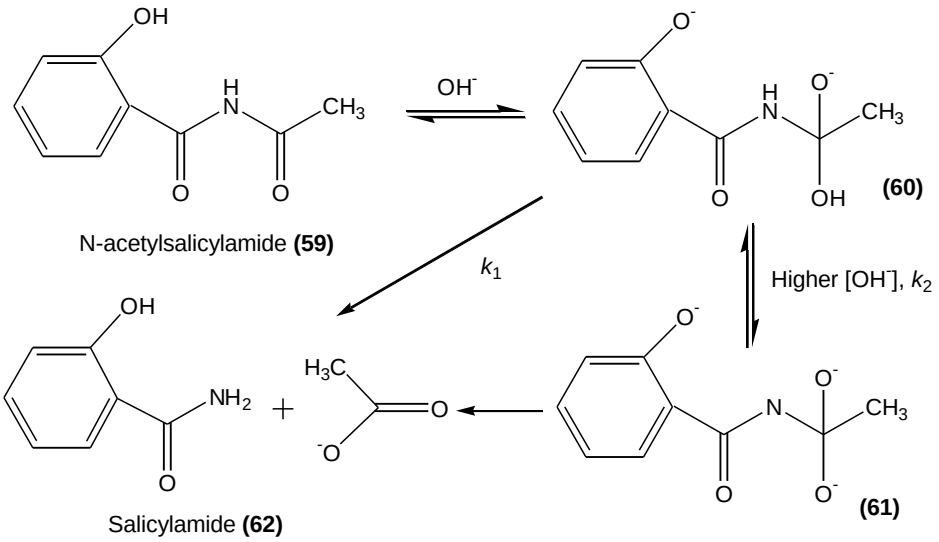

Figure 3-6: Hydrolysis of N-acetylsalicylamide

3.4 Measurement of first order rate constants for diacid amide hydrolysis at different pH's: Construction of a pH rate profile

Once that the rates for the ring-opening reaction had been measured, it was possible to move onto the final phase of the study: getting a full pH-rate profile for the hydrolysis reaction. As mentioned previously, no kinetic data have been compiled for an aryl amide of Kemp's acid, so plotting a full pH rate profile was of obvious interest for comparison with rate data for alkyl and aryl amides of Kemp's acid and also to determine the prodrug applicability of the synthesised Kemp's mono-ionised acid amide **(58)** at the pH differential between pH 5.8 and 7.3 and also absolute rate. The ionisation constants for both acid groups would also be sought from inflections in the pH rate profile (**Figure 3-2**) as long as the rates for non-

ionised and mono-ionised diacid amides were sufficiently different. In this context it was noticeable however, that Menger and Ladika observed only one apparent ionisation curve in the pH rate profile of their aliphatic diacid amide **(29)**.

The spectra were recorded over varying time intervals, from 40000 seconds for low pH analysis to 210000 seconds for high pH analysis. These time scales were chosen to incorporate at least 10 half-lives of the hydrolysis reaction. The analysis was conducted on a Hewlett-Packard Agilent 8453 UV/Vis spectrophotometer which as a diode-array instrument records full spectra at every pre-set time interval. Spectra and calculations were obtained with Agilent Chemstation software. The analysis was conducted using the first order kinetics method option in the software, which plots an exponential graph according to **equation 3**

$$a + b\, e^{(-kt)} \qquad \textbf{(equation 3)}$$

which allows k_{obs} (with standard deviation) to be calculated directly at any wavelength, the wavelengths of interest being 200 – 350 nm in this case, with a best fir curve fitted to data plotted as absorbance versus time. The absorbance data at 250 nm, where absorbance changes was at a maximum, were routinely used to calculate the rate constants. An example of a typical spectrum obtained by this analysis is shown in **Appendix II**. Other rate constants calculated using data from wavelengths in the 240 – 260 nm range always showed the same rate constants within experimental error.

Therefore the infinity data were not used because of over-emphasis on small absorbances at the late stages of the reaction in the curve fitting, but the analyses were conducted so that stable infinity values could be seen to ensure there was not any problem of drift which would affect the reaction rates calculated by the software.

Mono-potassium di-hydrogen phosphate and di-potassium hydrogen phosphate buffer solutions were used in varying ratios (**Table 3-3**) to make the buffers from pH 5.8 to 7.8. The lower the pH leads to increased rates of reaction as there is more un-ionised carboxylic acid groups which react intramolecularly to hydrolyse the amide (**section 1.4.6**).

For analysis at pH 4.5 – 5.8, mono-potassium ($HOOCCH_2COOK$) and di-potassium ($(KOOC)_2CH_2$) analogues of malonic acid were used. For lower pH analysis (pH 2.8 – 4.5), buffers were prepared by direct addition of excess malonic acid to KOH.

For the run at low pH (pH 0.5), standardised hydrochloric acid was added directly to boiled distilled water.

All of the rate constants obtained from these analyses were combined and plotted as log *k* versus pH to obtain a pH rate profile (**Figure 3-7**). A table of the calculated rate constants at each pH used to plot the pH rate profile can be found in **Appendix II**.

3.4.1 Buffer dilutions

Buffer solutions were normally used at 0.100 mol L^{-1} to ameliorate the effect of adding a high alkaline solution to start the reaction, even if only in small volumes. At this buffer concentration there was interest in what effect buffer catalysis may have on the rates of the hydrolysis reaction. Buffer catalysis is known to occur for some aryl amides with neighbouring carboxylate groups[51], so conducting a study on the possible effect that the buffer may have in this case was of obvious interest.

Buffer dilution analysis was carried out by halving or quartering the buffer concentration (in this case for the 1:1 phosphate buffer solution) and analysing the solution with half or a quarter as much of a regular injection of the ring-opened amide solution so that pH was retained. If no buffer catalysis was occurring, then there would be no change in the rate of reaction with concentration, but if buffer catalysis was occurring, then the rate would be of a lesser magnitude and the reaction rates for the other buffer solutions of full buffer concentration would have to be checked accordingly.

The resulting rates were found to be consistent with those calculated for solutions with full buffer concentration so buffer catalysis was not occurring to a measurable extent. The rate constants for the buffer dilutions are illustrated in **Figure 3-7**, with the red points indicating the rate constants of a two-fold buffer dilution (buffer concentration = 0.050 mol L^{-1})

and the purple points indicating the rate constants of a four-fold buffer dilution (buffer concentration = 0.0250 mol L^{-1}).

A buffer dilution run was also carried out on the 0.050:0.050 mol L^{-1} malonic acid solution to see if this showed any buffer catalysation. This involved a two-fold dilution which showed a negligibly higher rate constant than that observed for the full concentration run, which can be attributed to the diluted solution having a slightly lower pH, so buffer catalysis is not occurring for the malonic acid buffer solutions.

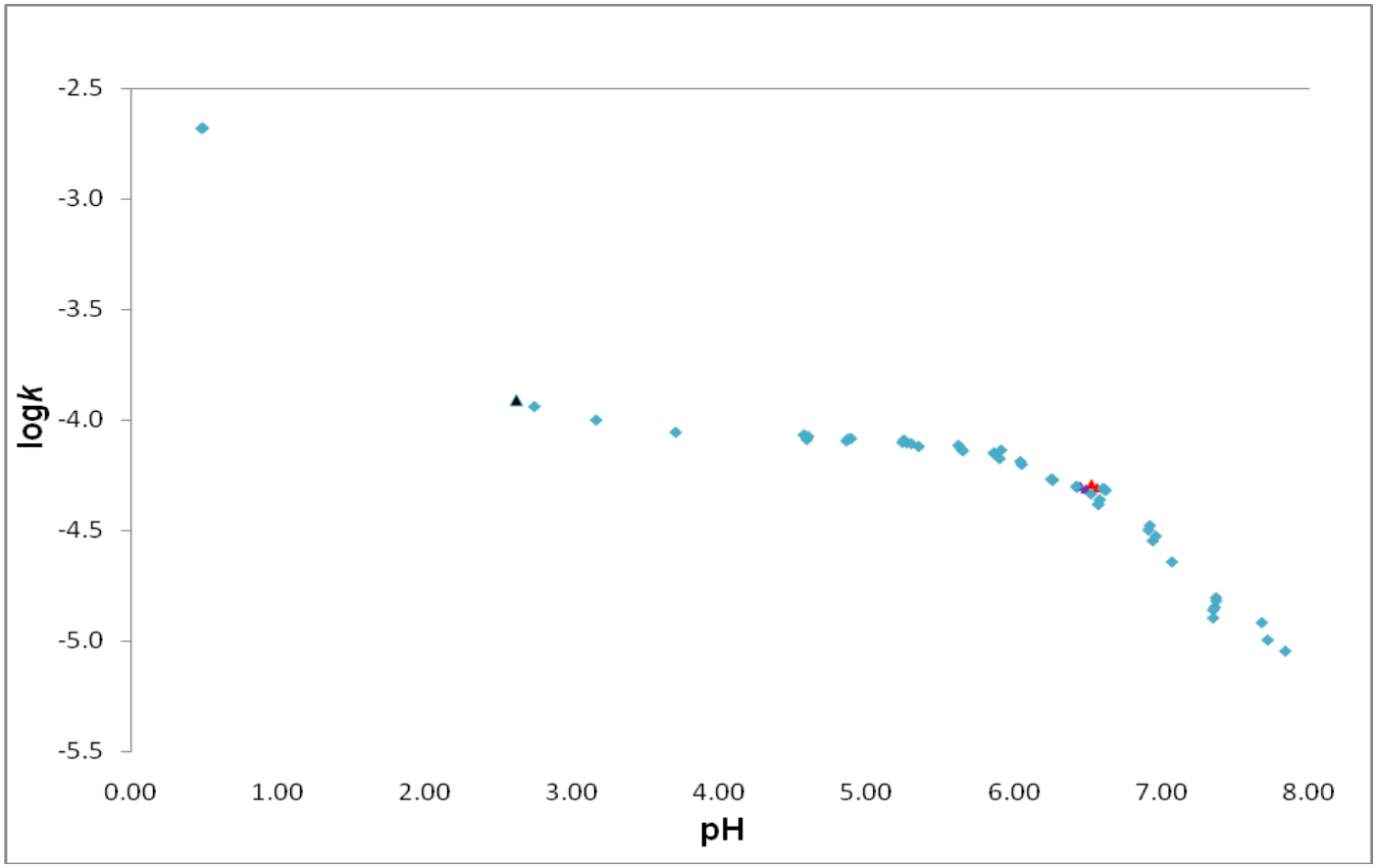

Figure 3-7: pH rate profile (log *k* versus pH) for the hydrolysis of the mono-ionised amide (phosphate buffer dilutions: red = ½ x buffer dilution, purple = ¼ x buffer dilution, malonic acid buffer dilution: black = ½ x buffer dilution)

3.4.2 Results

The pH rate profile (**Figure 3-7**) shows what appears to be a single ionisation curve at the pH of interest with respect to prodrug application. This corresponds to one carboxyl group being protonated and participating in the hydrolysis reaction. A plot of the type that Menger and Ladika[41] used to calculate the pK_a for their aliphatic amide is adapted in **Figure 3-8**. As only one carboxyl group participates in the hydrolysis reaction this plot can be analysed by **equation 4** (derivation of **equation 4** is shown in **Appendix III**):

$$1 / k_2 = (K_a / k_{lim} [H^+]) + 1 / k_{lim} \qquad \textbf{(equation 4)}$$

Where k_{lim} is the rate at 100% conjugate acid and K_a is the carboxylate group ionisation constant. As **equation 4** takes the form y = mx + c, a plot of $1 / k_2$ versus $1 / [H^+]$ will give an intercept of $1 / k_{lim}$ and slope of K_a / k_{lim}.

At pH below 2, there is seen to be a sharp increase in rate. The pH is too low for this to represent an increase corresponding to the ionisation of the second acid group. The same increase in reactivity below pH 2 was observed by Kluger and Lam,[51] and is most likely due to H^+ catalysation of the reaction.

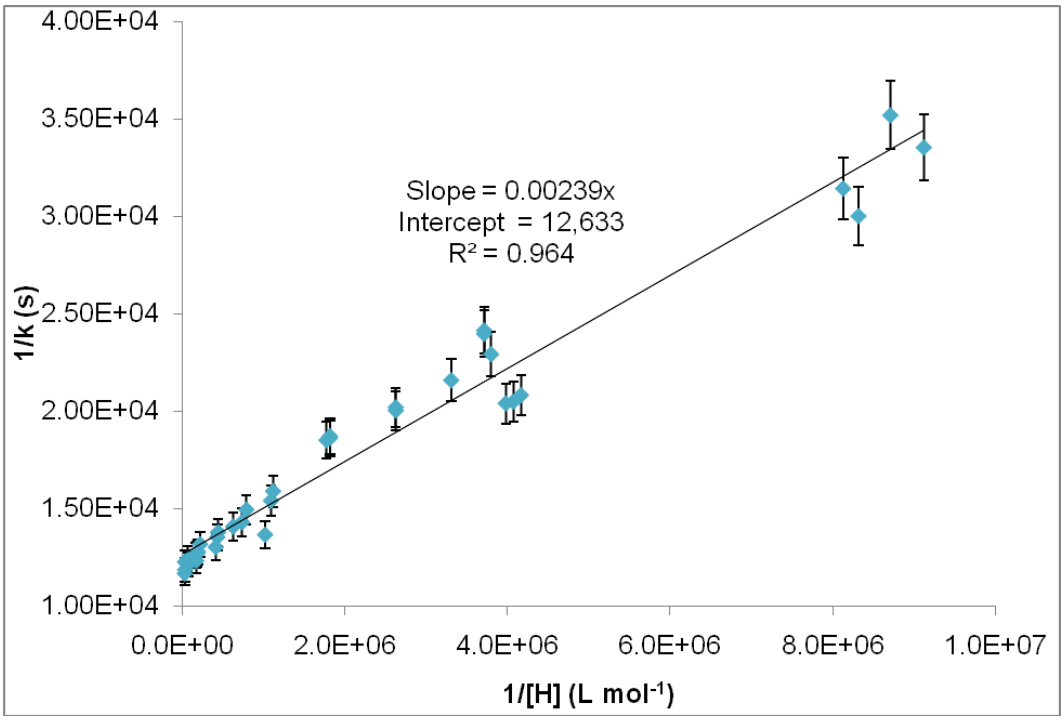

$$k_{lim} = 1 / \text{intercept} = (12633\ s)^{-1} = (7.9 \pm 0.8) \times 10^{-5}\ s^{-1}$$

$$\text{slope} = K_a / k_{lim},\ K_a = \text{slope} \times k_{lim} = (0.0024 \pm 0.00024)\ L\ mol^{-1} \times (7.9 \pm 0.8) \times 10^{-5}\ s^{-1}$$

$$= (1.9 \pm 0.4) \times 10^{-7}\ L\ mol^{-1}\ s^{-1}$$

$$pK_a = -\log K_a = -\log ((1.9 \pm 0.4) \times 10^{-7}\ L\ mol^{-1}\ s^{-1}) = 6.72 \pm 0.09$$

Data has assumed ± 10% error in the slope and intercept values

Figure 3-8: plot of 1/k versus 1/[H^+] over the pH range 4.5 – 7, data taken form **Figure 3-8** with assumed ± 5% error in 1/*k*, adapted from Menger and Ladika[41]

3.4.3 Discussion

3.4.3.1 Calculated pK_a value

The data over the pH range 4.5 – 7, are approximately linear, suggesting just one ionisation is operating, or if not, there is little difference in rate between the mono- and diacid forms. This coincidence is unexpected, except that similar was observed for aliphatic amide profiles,[41, 43] with no sign there either of the first ionisation down to pH 2, as likewise observed here.

Although there is no data is available for the ionisation constants of Kemp's acid, the pK_a value of 6.72 is high for an acid, and suggests that some stabilisation effect must be operating in the molecule to provide stability in a mono-ionised state. Such an interaction could be an interaction between the non-ionised carboxylate group and the ionised carboxylate group. This stabilisation factor could lead to the initial ionisation occurring easily as the mono-ionised state is in such a stable conformation. Similar systems such as that studied by Menger and Ladika show a pK_a value of 6.9 ± 0.4 for their tertiary alkyl amide **(29)**, based again on single ionisation analysis in the absence of any evidence for another low pH rate plateau.

3.4.3.2 Previous rate study comparisons

The reaction rates for the secondary amide compare well to the secondary aliphatic amide **(33b)** and secondary amide methyl ester **(35) (Figure 3-9)**

synthesised by Curran *et al*,[43] which had half-lives of 270 hours at pD 7 (22 ^{o}C) whilst at pH 6.6 (31.6 ^{o}C) the hydrolysis reaction for the mono-ionised amide acid **(58)** occurs with a half-life of just under four hours, a 67 fold faster reactivity difference. This is good evidence for the higher rate of reactivity of aryl compared to alkyl amides.

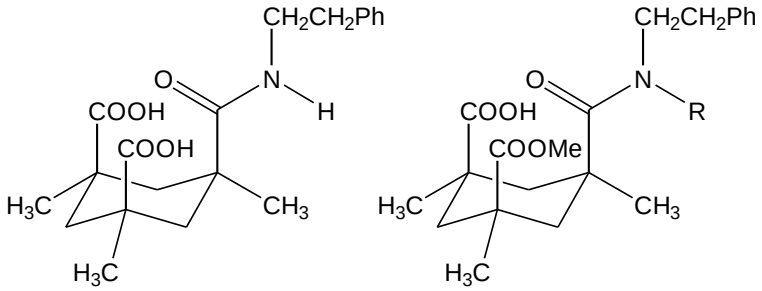

(33b) **(35)**

Figure 3-9: Two secondary amides synthesised by Curran *et al*[43]

Literature comparisons on the reactivity differences between secondary alkyl and aryl amides are scarce. One study that has been conducted was by Kirby and Lancaster[59] on substituted maleamic acids (**Figure 3-10**). The results of this study showed that the rate of amide hydrolysis from pH 0 – 5 for the aryl maleamic acid **(59a)** to be equal to 2.4 x 10^{-2} s^{-1}, six times higher than for the rate for the alkyl analogue **(59b)** which is equal to 3.9 x 10^{-3} s^{-1}. This difference in reactivity between aryl and alkyl amides suggests the likelihood of more generally higher rate of reaction of aryl amides compared to alkyl amides.

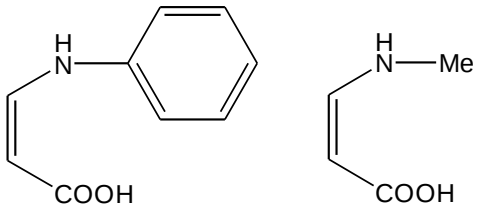

(59a) **(59b)**

Figure 3-10: Substituted maleamic acids studied by Kirby and Lancaster[59]

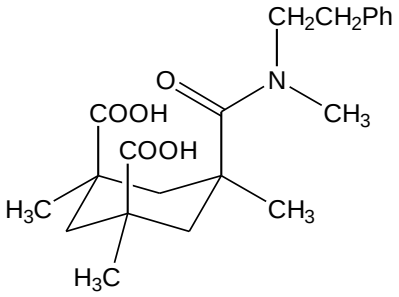

Figure 3-11: Tertiary amide **(33a)** studied by Curran *et al*[43]

The pseudoallylic strain proposed by Curran *et al*[43] for the high rate of reaction of the tertiary amide **(33a, Figure 3-11)** is unlikely to be occurring for the Kemp's mono-acid amide. For **(33a)** it is the presence of two bulky groups that cause the pseudoallylic strain, as the carbon to nitrogen bond can rotate to provide a conformation that has the least amount of steric strain. The least bulky methyl group on the tertiary amide nitrogen is situated close to the methyl group on the quaternary carbon in the ring structure preferentially over the larger alkyl group providing a conformation with the less amount of steric strain, however this conformation causes amide bond distortion due to the interaction between the two methyl groups, a distortion which is known to accelerate the rate of amide hydrolysis.[44] Such an interaction cannot occur for **(58)** as there is only one

bulky group on the amide nitrogen (in the form of the aromatic group) with the other group being a hydrogen, so the bond can rotate to move the less bulky hydrogen atom into a position which gives less steric strain. A possible interaction that may be occurring to retard the rate of hydrolysis in **(58)** could be a hydrogen bonding interaction between the amide hydrogen and the acid group, which would decrease the rate of reaction by rendering the amide carbonyl less able to react with the oxygen of the unionised carboxylic acid group which is needed to initiate anhydride formation and amine release (**Figure 3-12**).

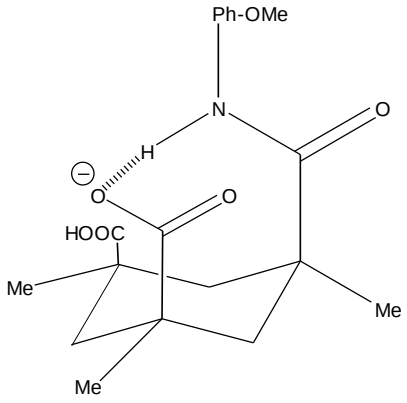

Figure 3-12: Possible interaction between amide hydrogen and an acid group in the Kemp's mono-ionised acid amide molecule **(58)**

3.4.3.3 Prodrug applicability and advantages (if any) of aryl vs. alkyl amides

With respect to prodrug applicability, the hydrolysis reaction shows a reactivity difference between pH 5.8 and pH 7, with a half-life of 506 minutes at pH 7.07 and a lower half-life of 162 minutes at pH 5.8, roughly one third as fast as at the higher pH. The half-life at the lower pH is too long for potential prodrug use at this stage, as ideal half-lives for prodrug

diffusion into cells in a tumour upon cytotoxin release have been calculated to be in the range of many seconds to a few minutes[60], as this allows for as many cytotoxic molecules as possible to attack the hypoxic cells, maximising the efficiency of a prodrug. Having such a high half life here would mean decreased efficiency and also could mean possible diffusion of the released active cytotoxin into normal healthy bodily tissues via the bloodstream.

The main hindrance to prodrug potential however, is the difference in reactivity at the two pHs of interest not being of a great enough magnitude, as by the time that three half-lives of the cytotoxin release had occurred at lower pH, the cytotoxin would also start to be released at higher pH throughout the rest of the body. Although the illustrated doxorubicin system **(41d)** had the same problem of low reactivity at lower pH (pH 5), it had a large difference in reactivity between pH 5 and pH 7, having a half-life of over 100 days at the higher pH, 60 times slower compared to the half-life at lower pH. This is the type of reactivity difference that would be ideal for any possible future application of prodrugs utilising the Kemp's acid scaffold.

The reaction rates of the tertiary and secondary amides synthesised by Curran *et al*[43] (**section 1.5.1**) showed rate differentials ranging over several orders of magnitude (from 10^2 – 10^4) slower for the secondary amide derivatives. Applying the lower differential in rate (10^2) to tertiary and secondary analogues of the mono-ionised Kemp's amide **(58)**, this

would mean a decrease in half-life from 162 minutes for a secondary amide at pH 5.8 to a possible half-life of one and a half minutes for a tertiary amide, a time which is much more suited to prodrug applicability. Applying the same hypothetical rate differential to the rate at higher pH (pH 7), the half-life time would decrease from 506 minutes to five minutes. Of course, this hypothetical comparison is reliant on the presence of the same pseudoallylic strain in a tertiary amide of Kemp's acid as there was in the molecules studied by Curran *et al*[43]. Also, the tertiary amides synthesised by Curran *et al*[43] were aliphatic, so comparison of aryl and aliphatic systems may be unreliable, but at least it gives some hope that the Kemp's acid system may be suited to prodrug applicability if tertiary amides can be synthesised. The rates of tertiary aryl amides may be even faster than in the comparisons illustrated above due to the faster overall reaction times of aryl systems compared to alkyl systems. These hypothetical reaction times are similar to those found for similar tertiary amides such as the amide studied by Glusenkamp *et al*[35] **(22a)** which had a half-life of 30 seconds at pH 6 and 2.4 minutes at pH 7, and are much better suited to the needs of a prodrug system.

From the evidence previously illustrated it seems that to get a molecule that is reactive enough at the lower pH of interest, a tertiary amide of Kemp's acid is needed. As touched on earlier in this discussion, the reaction rate of a tertiary aryl amide derivative could have a half-life of roughly a minute, an ideal time for prodrug use. Any possible structural

modifications that could be carried out are covered in the extensions and conclusions chapter below.

3.5 Experimental

3.5.1 Buffer and other solution preparations

Distilled water for buffer solution preparation was boiled under nitrogen flow for 30 minutes then cooled under nitrogen to remove all carbon dioxide. A soda lime tube was attached upon cooling to prevent any atmospheric carbon dioxide re-entering the solution. All glassware that was used was washed in an acid bath.

KOH to be used was standardised by titration with standard HCl using phenolphthalein as an indicator. It was found that a solution that was thought to be made to 0.200 mol L^{-1} has a true concentration of only 0.160 mol L^{-1}, so any further solution made with the KOH would have to contain 1.25 times as much KOH as originally calculated.

Kinetic studies were performed on a Hewlett-Packard Agilent 8354 diode-array spectrophotometer first order rate constants were calculated by the Agilent Chemstation software in the kinetics mode

3.5.2 Amide solution preparation and kinetic methods

The imide **(43)** (17 mg) was placed in 0.5 mL of 0.500 mol L^{-1} NaOH and reacted for 10 half-lives at 30 ^{o}C to ensure that the ring-opening reaction had gone to completion and the di-ionised acid amide group was present. To initiate the hydrolysis reaction a small volume of this solution (10 µL), was added to roughly 2.5 mL of 0.100 mol L^{-1} phosphate buffer solutions

of varying pH within a temperature pre-equilibrated silica cell in the spectrophotometer, and analysed in the UV/Vis spectrum between 200 - 350 nm. The scans showed the previously observed isosbestic point at 233 nm. The reaction was thermostatted at constant temperature.

For the buffer solutions, KCl, monopotassium dihydrogen phosphate and di-potassium hydrogen phosphate solutions (0.200 mol L^{-1}) were prepared by weight. Solid KCl was dried overnight in an oven and then the solid was added to 500 mL of the boiled water to make a 2.00 mol L^{-1} solution. The monopotassium dihydrogen phosphate solution was prepared by some of the solid to 100 mL of the boiled water. The di-potassium hydrogen phosphate was made by some of the solid to 100 mL of the boiled water.

pH 5.8 – 7.8 buffers were made up to 20 mL with combinations of monopotassium dihydrogen phosphate and di-potassium hydrogen phosphate solutions (0.200 mol L^{-1}). With KCl (2.00 mol L^{-1}) added in volumes sufficient to maintain the total ionic strength of solution at 1.00 mol L^{-1}. Finally, H_2O was added to make the volume up to 20 mL (**Table 3-3**). The ionic strength (μ) of the solution was calculated using **equation 5**:

$$\mu = \tfrac{1}{2} \Sigma (c_i z_i^2) \qquad \textbf{(equation 5)}$$

(where c_i = concentration of ion *i* in solution and z_i is the charge of *i* in solution), an example calculation is given below for a 0.100 mol L^{-1} phosphate buffer solution.

Table 3-2: Table of values used to prepare a 20 mL 1:1 phosphate buffer solution, with calculations for ionic strength (underlined values calculated as shown below)

Buffer species	Buffer concentration (mol L^{-1})	Volume (mL)	Ionic strength (μ, mol L^{-1})
KH_2PO_4	0.200	5	0.050
K_2HPO_4	0.200	5	0.150
KCl	2.00	8	0.80
H_2O	-	2	-

Using **equation 5:**

For KH_2PO_4: $\mu = ½ \Sigma ([K^+] \times 1^2) + ([H_2PO_4^-] \times 1^2) = ½ \Sigma (0.05 \text{ mol } L^{-1} \times 1^2) + (0.05 \text{ mol } L^{-1} \times 1^2) = ½ (0.10 \text{ mol } L^{-1}) = 0.050 \text{ mol } L^{-1}$

For K_2HPO_4: $\mu = ½ \Sigma (2 [K^+] \times 1^2) + ([HPO_4^{2-}] \times 2^2) = ½ \Sigma ((2 \times 0.05 \text{ mol } L^{-1}) \times 1^2) + (0.05 \text{ mol } L^{-1} \times 2^2) = ½ (0.30 \text{ mol } L^{-1}) = 0.150 \text{ mol } L^{-1}$

Combining the two values gives a contribution of 0.20 mol L^{-1} from the buffer species towards the overall ionic strength. Therefore 0.8 μ is needed from KCl to make the ionic strength equal to 1 mol L^{-1}.

So 8 mL of 2.00 mol L^{-1} KCl diluted in the 20 mL will bring the ionic strength to 1 mol L^{-1}, as:

$$\mu = (8 \text{ mL} / 20 \text{ mL}) \times 2 \text{ mol } L^{-1} = 0.8 \text{ mol } L^{-1}$$

The remaining 2 mL needed to make the solution up to 20 mL comes from using the boiled distilled water.

Table 3-3: Table of volumes used to make 20 mL phosphate buffer solutions for pH 5.8 to 7.8 analysis (all volumes in mL)

Buffer ratios (KH_2PO_4 : K_2HPO_4)	**KH_2PO_4 (0.200 mol L^{-1})**	**K_2HPO_4 (0.200 mol L^{-1})**	**KCl (2.00 mol L^{-1})**	**H_2O**
1 : 9	1	9	7.2	2.8
1 : 7	1.25	8.75	7.25	2.75
1 : 3	2.5	7.5	7.5	2.5
1 : 1	5	5	8	2
3 : 2	6	4	8.2	1.8
3 : 1	7.5	2.5	8.5	1.5
4 : 1	8	2	8.6	1.4

For pH analyses from pH 4.5 to 5.8, malonic acid buffers were used. By adding different amounts of the malonic acid to KOH, different ionisations states of the malonic acid could be obtained. 2.081 g (0.0200 mol) of the malonic acid was added to 20 mL of KOH (1.00 mol L^{-1}) and made up to 100 mL with KCl (2.00 mol L^{-1}) yielding the mono-potassium dihydrogen malonic acid ($HOOCCH_2COOK$) (0.0200 mol L^{-1}). Adding the same amount (0.0200 mol) of malonic acid to 40 mL of KOH and making up to 100 mL with KCl yielded the di-potassium hydrogen malonic acid

($(KOOC)_2CH_2$) (0.0200 mol L^{-1}). As for the phosphate buffer solutions, combining these two buffer solutions in different ratios meant that different pHs could be achieved. KCl was again added in volumes sufficient to maintain the ionic strength at 1 mol L^{-1}, with the boiled water added to make the solution up to 20 mL (**Table 3-4**).

Table 3-4: Table of volumes used to make 20 mL malonic acid buffer solutions for pH 4.5 – 5.8 analysis (all volumes in mL)

Buffer ratios ($HOOCCH_2COOK$: ($(KOOC)_2CH_2$)	**$HOOCCH_2COOK$ (0.0200 mol L^{-1})**	**$(KOOC)_2CH_2$ (0.0200 mol L^{-1})**	**KCl (2.00 mol L^{-1})**	**H_2O**
2 : 3	4	6	7.8	2.2
1 : 1	5	5	8	2
3 : 2	6	4	8.2	1.8
3 : 1	7.5	2.5	8.5	1.5
9 : 1	9	1	8.8	1.2

For pH analysis at pH 2.7 - 4.5, a constant amount of malonic acid solid (0.2081g, 0.05 mol) was added directly to varying concentrations of KOH with the ionic strength maintained at 1 mol L^{-1} by addition of KCl. Finally H_2O was added to make up the volume to 20 mL.

Table 3-5: Table of volumes used to make 20 mL buffer solutions for low pH (4.5 – 2.7 pH) analysis (all volumes in mL)

$HOOCCH_2COOK$ Concentration (mol L^{-1})	**$(KOOC)_2CH_2$ concentration (mol L^{-1})**	**Volume KOH (1.00 mol L^{-1})**	**Volume KCl (2.00 mol L^{-1})**	**Volume H_2O**
0.0500	-	1	9	10
0.0300	0.0200	1.4	8.6	10
0.0100	0.0400	1.8	8.2	10

For the run at very low pH (pH 0.5), a 1 mol L^{-1} HCl run was used. To prepare this buffer solution, standardised HCl (1.014 mol L^{-1}, 8.85 mL) was added to boiled distilled water (11.15 mL) to make a 20 mL volume.

3.5.2.1 Buffer dilutions

For a two-fold dilution of the phosphate buffer, the buffer concentration was reduced to 0.050 mol L^{-1} and 5 µL of the ring-opened imide solution was injected. For a four-fold dilution the concentration was reduced to 0.0250 mol L^{-1} and 2.5 µL of the ring-opened amide solution was added.

For a two-fold dilution of the malonic acid solution, the buffer concentration was reduced to 0.0250 mol L^{-1} and 5 µL of the ring-opened imide solution was injected.

4 Conclusions and project extension

4.1 Extension: suggestions for future research

As mentioned previously, the synthesis of a tertiary amide of Kemp's acid would be of great interest with regard to prodrug applicability, now that the reactivity of an aryl amide of Kemp's acid has been shown to be greater than that of a like alkyl amide. Also documented, in chapter two, are the attempts at trying to synthesise such a tertiary amide from methods present in the literature, attempts which failed to produce any of the desired product. Another option available is direct conversion of the secondary amide into a tertiary amide. There are many methods for both alkylation and acylation of the amide nitrogen at acidic,[61] neutral and basic conditions, which are extensively reviewed.[62, 63] For the Kemp's system, the conversion into a tertiary amide would have to occur at higher pH, as this is where the amide is in its stable dianionic form **(44)**. Also, as the amide at higher pH is in a molecule that has already two ionised carboxylate groups, a strong base would also be needed to deprotonate the amide nitrogen.

Changing the structure from a secondary to a tertiary amide will however most likely not change the pK_a values to much extent, so the relative rates at ph 5.8 versus pH 7 would be similar still and rate difference would most likely need adjustment. The *cis,trans* secondary amide **(37b)** synthesised

by Curran *et al*[43] showed a pK_a value of 4.39, which is lower than that of the *cis,cis* isomer **(33b)** which had a pK_a of 5.45. Thus possible modification of one of the axial groups on the Kemp's amide molecule could result in a decrease in pK_a, such that the relative rates of reactivity in the required pH sensitivity zone would be larger.

One method of amide conversion is outlined in **Figure 4-1**, where a secondary aryl amide **(60)** is converted to a tertiary aryl amide **(61)** using sodium amide as a strong base and then reacting the deprotonated amide with an electrophile. This reaction had a good yield of 67.5 %.[64]

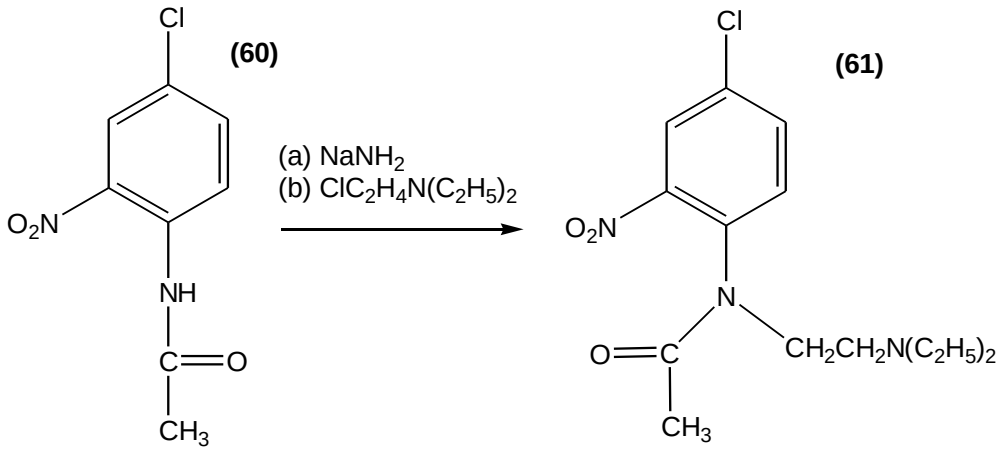

Figure 4-1: Conversion of a secondary amide to tertiary amide

Following a synthesis of an amide of Kemp's acid with high enough rate of reactivity, the next logical step in an extension would be the attachment of a cytotoxic species. A molecule that could be attached is one previously studied by Kelly[65] and also Atwell *et al*[66]. This research was concerned with the synthesis of a *seco*-cyclopropylbenzindoline (CBI) **(64)** prodrug by attaching an indole effector **(62)** to a *gem*-dimethylated acid **(63) (Figure**

4-2). The R group on **(62)** was varied as shown in **Table 4-1**, which showed that the group with the greatest cytotoxicity is that with an NHMe at the R position. The effect of the R group on toxicity can be seen from the table, with a 4000 fold range of cytotoxicity observed for the four analogues. The synthesis of this molecule was achieved under relatively easy conditions, although purification was an issue and a small yield of 15% was obtained. The obvious potential of the molecule **(62b)** cannot be ignored, and so possible attachment of this molecule to the Kemp's acid scaffold would be of great interest.

Table 4-1: Growth inhibition of AA8 cells, following four hour drug exposure[66]

Compound	R group	IC50 (nM)
62a	NO_2	1600 ± 500
62b	NH_2	0.43 ± 0.05
62c	NHMe	0.17 ± 0.02
62d	NMe_2	5.6 ± 0.6

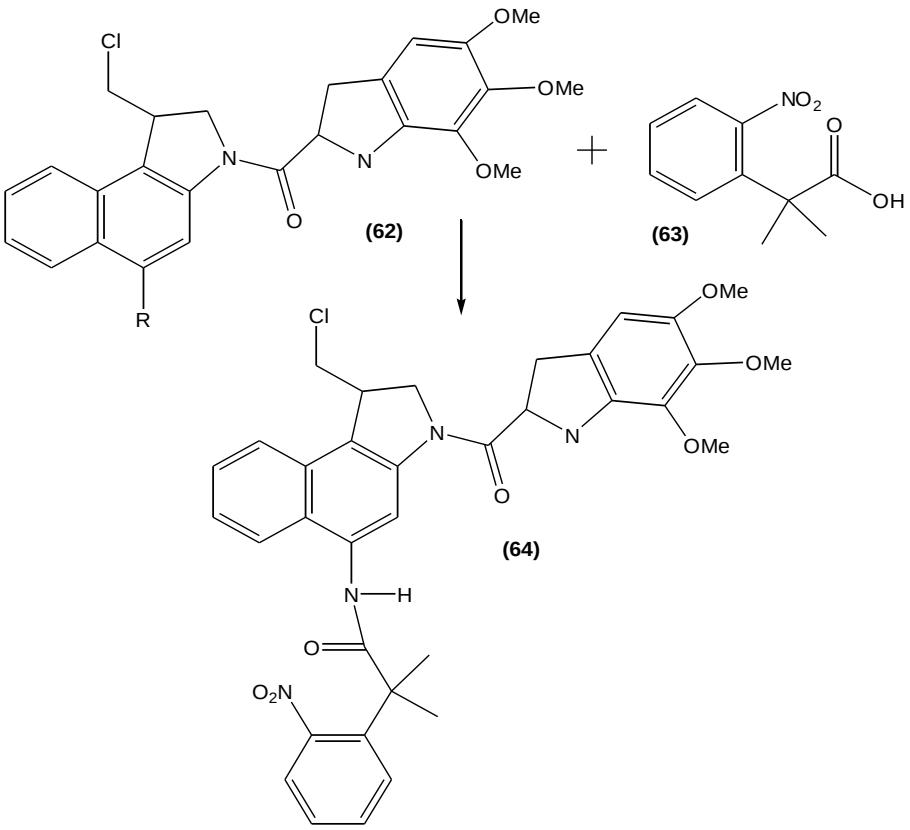

Figure 4-2: Synthesis of a CBI prodrug **(64)**

Another potential cytotoxin that could be utilised on the Kemp's acid scaffold is that of doxorubicin. The doxorubicin system illustrated in **section 1.5.2** shows good potential for prodrug applicability, and has already been attached to the Kemp's acid scaffold, so further research using this molecule would be relatively simple. The researchers of the doxorubicin system did not give any reason as to why the huge rate differential was observed between pH 5 and 7 for the secondary amides **(41b)** and **(41d)**, as well as why the tertiary amide **(41c)** had such a retarded rate of reaction. Also testing the reactivity of these compounds at the slightly higher pH of 6 would be of interest as this is the pH with respect to prodrug applicability.

4.2 Summary and conclusions

The pH rate profile of the Kemp's secondary amide **(58)** fits a model of neighbouring group catalysis by a single non-ionised group, with a limiting rate constant at lower pH of 7.9 x 10^{-5} s^{-1}, and a calculated pK_a of 6.72. This pK_a value is in good agreement with that calculated by Menger and Ladika[41] for their tertiary pyrrolidyl amide, which had a pK_a of 6.9. The calculations used to derive these pK_a values are subject to some uncertainty due to the absence of a different limiting plateau for the neutral amide di-acid at lower pH which if it were apparent and extricable from the higher pH data might have allowed some correction to k_{lim} and pK_a for the mono-ionised acid amide **(58)**.

Irrespective of the difficulty with quantitative interpretation, the rate of amine release from the prodrug model at extracellular tumour pH of 5.8 had a half-life of 162 minutes compared with a half-life of 502 minutes at pH 7 (taken to be the normal intracellular pH), a roughly three fold difference in reactivity. This reactivity difference is not large enough however for any potential prodrug application at this stage. The type of reactivity difference that is needed is of greater magnitude, so that the molecule is highly stable for a long period of time in the body at large, as this would decrease the possibility of side-effects occurring. This difference in reactivity, and also the overall speed of the reaction is too slow for potential prodrug applicability (Denny calculated a diffusion time of seconds to a few minutes upon prodrug activation in a tumour for

maximum effect[60]). Thus this secondary amide of Kemp's acid is not suited to prodrug applications.

As discussed, tertiary amides of Kemp's acid (such as **29**, **31**, **33a** and **37a**, as discussed in **section 1.5.1**) have higher relative rates to that of similar secondary amides, due to strain effects present in the structure of the tertiary amide molecules. Therefore, for further studies on Kemp's acid, it seems the most fruitful path for further prodrug related research would be that of conversion of the secondary amide to a tertiary amide. Many such methods are available in the literature, and some are discussed previously in **section 4.1**.

However, such a conversion to a tertiary amide would not significantly alter the pK_a value for the second dissociation constant, which is too high for large enough rate discrimination. Structural modifications on the Kemp's scaffold could be envisaged such as that done on the doxorubicin system **(41c)** in **section 1.5.2**, where the R group on the amide nitrogen was varied, although to limited effect. This structural modification would be initiated with the goal of lowering the pK_a but increasing the absolute rate of reaction to compensate for the effect of lower pK_a on absolute rate at pH 5.8 versus 7 would be a useful target.

Appendix I

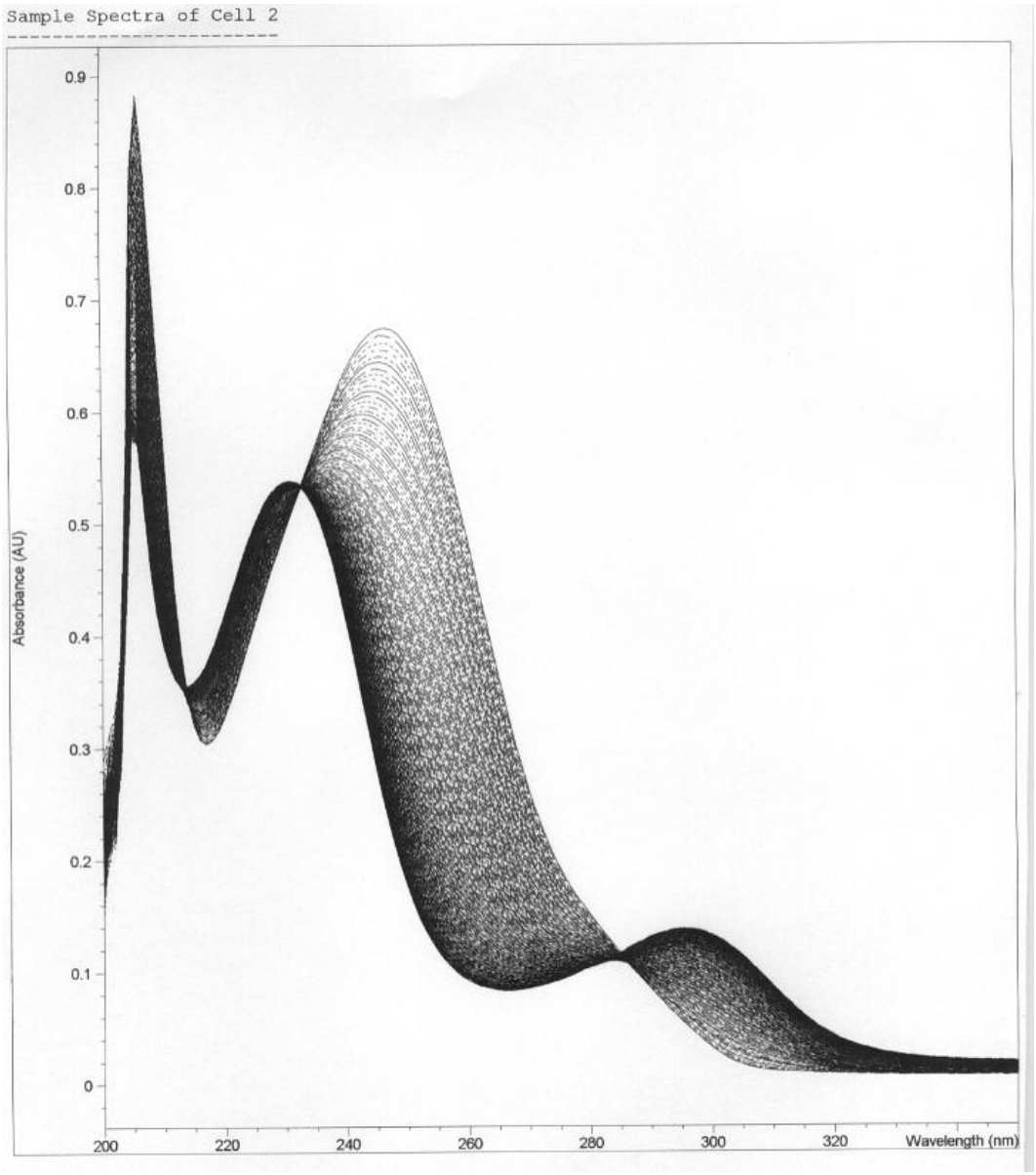

Plot of absorbance versus wavelength (nm) for a 1:1 phosphate buffer run (note the observed isosbestic point at 233 nm)

Appendix II

Table of data used to plot the pH rate profile (Figure 3-7)

Buffer solution ratio	pH	k (s^{-1})	Error in k (s^{-1})
KH_2PO_4 : K_2HPO_4			
1 : 9	7.84	8.99×10^{-6}	4.0×10^{-7}
1 : 9	7.72	1.01×10^{-5}	1.0×10^{-6}
1 : 9	7.68	1.21×10^{-5}	1.3×10^{-6}
1 : 7	7.37	1.52×10^{-5}	6.6×10^{-7}
1 : 7	7.37	1.57×10^{-5}	9.4×10^{-7}
1 : 7	7.36	1.42×10^{-5}	3.6×10^{-7}
1 : 7	7.35	1.38×10^{-5}	3.0×10^{-7}
1 : 7	7.35	1.27×10^{-5}	3.6×10^{-7}
1 : 3	7.07	2.28×10^{-5}	6.6×10^{-7}
1 : 3	6.96	2.98×10^{-5}	1.1×10^{-6}
1 : 3	6.94	2.83×10^{-5}	8.9×10^{-7}
1 : 3	6.92	3.33×10^{-5}	1.2×10^{-6}
1 : 3	6.91	3.18×10^{-5}	8.4×10^{-7}
1 : 1	6.62	4.80×10^{-5}	6.5×10^{-7}
1 : 1	6.61	4.88×10^{-5}	5.6×10^{-7}
1 : 1	6.6	4.90×10^{-5}	6.2×10^{-7}
1 : 1	6.58	4.36×10^{-5}	9.6×10^{-7}
1 : 1	6.57	4.17×10^{-5}	3.3×10^{-6}
1 : 1	6.57	4.14×10^{-5}	6.9×10^{-7}

1 : 1	6.52	4.63×10^{-5}	4.3×10^{-7}
1 : 1	6.42	4.95×10^{-5}	7.8×10^{-7}
1 : 1	6.42	4.99×10^{-5}	9.1×10^{-7}
1 : 1 (½ x buffer dilution)	6.56	4.96×10^{-5}	1.6×10^{-6}
1 : 1 (½ x buffer dilution)	6.52	5.15×10^{-5}	1.8×10^{-6}
1 : 1 (¼ x buffer dilution)	6.48	4.89×10^{-5}	1.3×10^{-5}
1 : 1 (¼ x buffer dilution)	6.45	5.00×10^{-5}	1.7×10^{-5}
3 : 2	6.26	5.34×10^{-5}	1.5×10^{-6}
3 : 2	6.26	5.37×10^{-5}	2.4×10^{-6}
3 : 2	6.25	5.40×10^{-5}	3.1×10^{-6}
3 : 1	6.05	6.29×10^{-5}	4.2×10^{-7}
3 : 1	6.04	6.49×10^{-5}	7.3×10^{-7}
4 : 1	5.91	7.32×10^{-5}	1.3×10^{-6}
4 : 1	5.9	6.69×10^{-5}	8.4×10^{-7}
4 : 1	5.87	6.99×10^{-5}	4.8×10^{-7}
4 : 1	5.86	7.1×10^{-5}	4.5×10^{-7}
$HOOCCH_2COOK$: $(KOOC)_2CH_2$			
2 : 3	5.65	7.25×10^{-5}	2.6×10^{-6}
2 : 3	5.64	7.29×10^{-5}	3.4×10^{-6}
2 : 3	5.62	7.68×10^{-5}	3.8×10^{-6}
1 : 1	5.35	7.59×10^{-5}	4.3×10^{-7}

1 : 1	5.30	7.82×10^{-5}	5.1×10^{-7}
3 : 2	5.27	7.88×10^{-5}	7.3×10^{-7}
3 : 2	5.25	8.12×10^{-5}	1.0×10^{-6}
3 : 2	5.24	7.92×10^{-5}	8.4×10^{-7}
3 : 1	4.89	8.25×10^{-5}	2.5×10^{-6}
3 : 1	4.87	8.04×10^{-5}	2.1×10^{-6}
3 : 1	4.86	8.20×10^{-5}	1.4×10^{-6}
9 : 1	4.6	8.43×10^{-5}	1.8×10^{-6}
9 : 1	4.59	8.16×10^{-5}	6.0×10^{-7}
9 : 1	4.57	8.57×10^{-5}	8.8×10^{-7}
Solid malonic acid runs			
$HOOCCH_2COOK$: $(KOOC)_2CH_2$			
0.010 : 0040 mol L^{-1}	3.70	8.80×10^{-5}	1.4×10^{-6}
0.030 : 0.020 mol L^{-1}	3.16	1.00×10^{-4}	1.4×10^{-6}
0.050 : 0 mol L^{-1}	2.74	1.15×10^{-4}	1.0×10^{-6}
0.050 : 0 mol L^{-1} (½ x buffer dilution)	2.62	1.22×10^{-4}	2.0×10^{-6}
1 mol L^{-1} HCl runs			
1 mol L^{-1} HCl	0.49	2.10×10^{-3}	1.3×10^{-5}
1 mol L^{-1} HCl	0.48	2.09×10^{-3}	1.0×10^{-5}

Appendix III

Derivation of the linear relationship between 1 / *k* and 1 / [H^+] used to obtain k_{lim} and K_a (equation 4, page 70)

$$1 / k_2 = (K_a / k_{lim} [H^+]) + 1 / k_{lim} \qquad \textbf{(equation 4)}$$

k_{lim} is the rate for acid at 100 % conjugate acid (in the case of this application this term represents the fully protonated amide mono-anion **(58)**), assuming no reaction of ionised acid group form (in this case the di-ionised amide **(44)**, which is known to be stable at pH 12). Since the observed rate constant will depend on the fraction of amide in the reactive (mono) acidic form,

$$k_{obs} = f \times k_{lim} \qquad \textbf{(equation 6)}$$

where f is the fraction of the reactive acid form:

$$f = [RCOOH] / ([RCOOH] + [RCOO^-])$$

$$1 / f = ([RCOOH] + [RCOO^-]) / [RCOOH]$$

$$= 1 + [RCOO^-] / [RCOOH] \qquad \textbf{(equation 7)}$$

The dissociation constant K_a is given by:

$$K_a = [RCOO^-] [H_3O^+] / [RCOOH]$$

whereby:

$$[RCOO^-] / [RCOOH] = K_a / [H_3O^+]$$

Inserting this term into **equation 7** we get:

$$1 / f = 1 + K_a / [H_3O^+] \qquad \textbf{(equation 8)}$$

From **equation 6**:

$$k_{obs} = f \times k_{lim}$$

$$1 / k_{obs} = (1 / f) \times (1 / k_{lim})$$

Inserting **equation 8** into this expression yields:

$$1 / k_{obs} = (1 + K_a / [H_3O^+]) \times 1 / k_{lim}$$

$$= K_a / k_{lim} \times 1 / [H_3O^+] + 1 / k_{lim}$$

Simplifying this equation gives **equation 4**:

$$1 / k_{obs} = K_a / k_{lim} [H_3O^+] + 1 / k_{lim} \qquad \textbf{(equation 4)}$$

References

1. Maugh, T. H.; Marx, J. L., *Seeds of destruction*. Plenum: New York, 1975.

2. World Health Organization. Cancer fact sheet. http://www.who.int/mediacentre/factsheets/fs297/en/ (July 1, 2009),

3. Avendaño, C.; Menéndez, J. C., *Medicinal chemistry of anticancer drugs*. Elsevier: Amsterdam, 2008.

4. Altman, R.; Sarg, M. J., *The cancer dictionary: revised edition*. Checkmark: New York, 2000.

5. Nowell, P. C., The Clonal Evolution of Tumor Cell Populations. *Science* **1976,** 194, 23-28.

6. Merlo, L. M. F.; Pepper, J. W.; Reid, B. J.; Maley, C. C., Cancer as an evolutionary and ecological process. *Nature Reviews Cancer* **2006,** 6, 924-935.

7. Crespi, B.; Summers, K., Evolutionary biology of cancer. *Trends in Ecology & Evolution* **2005,** 20, 545-552.

8. Hartwell, L. H.; Kastan, M. B., Cell cycle control and cancer. *Science* **1994,** 266, 1821-1828.

9. Hanahan, D.; Weinberg, R. A., The Hallmarks of Cancer. *Cell* **2000,** 100, 57-70.

10. Doll, R.; Hill, A. B., Smoking and Carcinoma of the Lung. *British Medical Journal* **1950,** 2, 739-748.

11. Biesalski, H. K.; De Mesquita, B. B.; Andrew, C.; Chytil, F.; Grimble, R.; Hermus, R. J. J.; Köhrle, J.; Lotan, R.; Norpoth, K.; Pastorino, U.; Thurnham, D., European Consensus Statement on Lung Cancer: Risk factors and prevention. Lung Cancer Panel. *CA: A Cancer Journal for Clinicians* **1998,** 48, 167-176.

12. Sasco, A. J.; Secretan, M. B.; Straif, K., Tobacco smoking and cancer: a brief review of recent epidemiological evidence. *Lung Cancer* **2004,** 45, (Supplement 2), S3-S9.

13. O'Reilly, K. M. A.; McLaughlin, A. M.; Beckett, W. S.; Sime, P. J., Asbestos-related lung disease. *American Family Physician* **2007,** 75, 656-665.

14. English, D. R.; Armstrong, B. K.; Kricker, A.; Fleming, C., Sunlight and Cancer. *Cancer Causes & Control* **1997,** 8, 271-283.

15. Pagano, J. S.; Blaser, M.; Buendia, M.-A.; Damania, B.; Khalili, K.; Raab-Traub, N.; Roizman, B., Infectious agents and cancer: criteria for a causal relation. *Seminars in Cancer Biology* **2004,** 14, 453-471.

16. Walboomers, J. M. M.; Jacobs, M. V.; Manos, M. M.; Bosch, F. X.; Kummer, J. A.; Shah, K. V.; Snijders, P. J. F.; Peto, J.; Meijer, C. J. L. M.; Muñoz, N., Human papillomavirus is a necessary cause of invasive cervical cancer worldwide. *The Journal of Pathology* **1999,** 189, 12-19.

17. Croce, C. M., Oncogenes and Cancer. *The New England Journal of Medicine* **2008,** 358, 502-511.

18. Baker, S. J.; Fearon, E. R.; Nigro, J. M.; Hamilton, S. R.; Preisinger, A. C.; Jessup, J. M.; vanTuinen, P.; Ledbetter, D. H.; Barker, D. F.; Nakamura, Y.; White, R.; Vogelstein, B., Chromosome 17 deletions and p53 gene mutations in colorectal carcinomas. *Science* **1989,** 244, 217-221.

19. Kastan, M. B.; Zhan, Q.; El-Deiry, W. S.; Carrier, F.; Jacks, T.; Walsh, W. V.; Plunkett, B. S.; Vogelstein, B.; Fornace, A. J., A mammalian cell cycle checkpoint pathway utilizing p53 and GADD45 is defective in ataxia-telangiectasia. *Cell* **1992,** 71, 587-597.

20. Donehower, L. A.; Harvey, M.; Slagle, B. L.; McArthur, M. J.; Montgomery, C. A.; Butel, J. S.; Allan, B., Mice deficient for p53 are developmentally normal but susceptible to spontaneous tumours. *Nature* **1992,** 356, 215-221.

21. Sawyers, C., Targeted cancer therapy. *Nature* **2004,** 432, 294-297.

22. Folkman, J., Angiogenesis. *Annual Review of Medicine* **2006,** 57, 1-18.

23. Zetter, B. R., Angiogenesis and tumour metastasis. *Annual Review of Medicine* **1998,** 48, 407-24.

24. Thomlinson, R. H.; Gray, L. H., The histological structure of some human lung cancers and the possible implications for radiotherapy. *British Journal of Cancer* **1955,** 9, 539-549.

25. Brown, J. M.; Wilson, W. R., Exploiting tumour hypoxia in cancer treatment. *Nature Reviews Cancer* **2004,** 4, 437-447.

26. Harrison, L. B.; Chadha, M.; Hill, R. J.; Hu, K.; Shasha, D., Impact of Tumor Hypoxia and Anemia on Radiation Therapy Outcomes. *Oncologist* **2002,** 7, 492-508.

27. Denny, W. A., Prodrug strategies in cancer therapy. *European Journal of Medicinal Chemistry* **2001,** 36, 577-595.

28. Vaupel, P.; Schlenger, K.; Knoop, C.; Hockel, M., Oxygenation of Human Tumors: Evaluation of Tissue Oxygen Distribution in Breast Cancers by Computerized O2 Tension Measurements. *Cancer Research* **1991,** 51, 3316-3322.

29. Vaupel, P. W.; Frinak, S.; Bicher, H. I., Heterogeneous Oxygen Partial Pressure and pH Distribution in C3H Mouse Mammary Adenocarcinoma. *Cancer Research* **1981,** 41, 2008-2013.

30. Tannock, I. F.; Rotin, D., Acid pH in Tumors and Its Potential for Therapeutic Exploitation. *Cancer Research* **1989,** 49, 4373-4384.

31. Albert, A., Chemical aspects of selective toxicity. *Nature* **1958,** 182, 421-423.

32. Denny, W. A., The design of selectively-activated prodrugs for cancer chemotherapy. *Current pharmaceutical design* **1996,** 2, 281-294.

33. Eilat, E.; Arad-Yellin, R. Acid labile prodrugs. U.S. Patent 6,030,997, Feb. 29, 2000.

34. Tietze, L. F.; Neumann, M.; Mollers, T.; Fischer, R.; Glusenkamp, K.-H.; Rajewsky, M. F.; Jahde, E., Proton-mediated Liberation of Aldophosphamide from a Nontoxic Prodrug: A Strategy for Tumor-selective Activation of Cytocidal Drugs. *Cancer Research* **1989,** 49, 4179-4184.

35. Glüsenkamp, K. H.; Mengede, C.; Drosdziok, W.; Jähde, E.; Rajewsky, M. F., Rapid hydrolysis of amides under physiological conditions: Influence of the microenvironment on the stability of the amide bond. *Bioorganic & Medicinal Chemistry Letters* **1998,** 8, 285-288.

36. Dillman, R. O.; Johnson, D. E.; Shawler, D. L.; Koziol, J. A., Superiority of an Acid-Labile Daunorubicin-Monoclonal Antibody Immunoconjugate compared to Free Drug. *Cancer Research* **1988,** 48, 6097-6102.

37. Billett, G. B.; Phillis, A. T.; Main, L.; Nicholson, B. K.; Denny, W. A.; Hay, M. P., The 3-*N*-phenyl amide of *all-cis*-cyclopentane-1,2,3,4-tetracarboxylic acid as a potential pH-sensitive amine-releasing prodrug; intervention of imide formation around neutral pH. *ARKIVOC* **2006,** iii, 184-201.

38. Kemp, D. S.; Petrakis, K. S., Synthesis and Conformational Analysis of *cis-cis*-1,3,5-trimethylcyclohexane-1,3,5-tricarboxylic acid. *Journal of Organic Chemistry* **1981,** 46, 5140-5143.

39. Rebek, J., Jr.; Marshall, L.; Wolak, R.; Parris, K.; Killoran, M.; Askew, B.; Nemeth, D.; Islam, N., Convergent functional groups: Synthetic and structural studies. *Journal of the American Chemical Society* **1985,** 107, 7476-7481.

40. Onoda, A.; Haruna, H.; Yamamoto, H.; Takahashi, K.; Kozuki, H.; Okamura, T.-a.; Ueyama, N., Proton-driven Conformational switch of a cyclohexyl skeleton coupled with NH--O hydrogen-bond formation. *European Journal of Organic Chemistry* **2005**, 641-645.

41. Menger, F. M.; Ladika, M., Fast hydrolysis of an aliphatic amide at neutral pH and ambient temperature. A peptidase model. *Journal of the American Chemical Society* **1988,** 110, 6794-6796.

42. Dunitz, J. D., *X-ray Analysis and the Structure of Organic Molecules*. Cornell University press: Ithaca, 1979.

43. Curran, T. P.; Borysenko, C. W.; Abelleira, S. M.; Messier, R. J., Intramolecular acylolysis of amide derivatives of Kemp's triacid: strain effects and reaction rates. *Journal of Organic Chemistry* **1994,** 59, 3522-3529.

44. Bennet, A. J.; Wang, Q. P.; Slebocka-Tilk, H.; Somayaji, V.; Brown, R. S.; Santarsiero, B. D., Relationship between amidic distortion and ease of hydrolysis in base. If amidic resonance does not exist, then what accounts for the accelerated hydrolysis of distorted amides? *Journal of the American Chemical Society* **1990,** 112, 6383-6385.

45. Dougan, M. L.; Chin, J. L.; Solt, K.; Hansen, D. E., Rapid cleavage of cyclic tertiary amides of Kemp's triacid: effects of ring structure. *Bioorganic & Medicinal Chemistry Letters* **2004,** 14, 4153-4156.

46. Gerschler, J. J.; Wier, K. A.; Hansen, D. E., Amide bond cleavage: Acceleration due to a 1,3 diaxial interaction with a carboxylic acid. *Journal of Organic Chemistry* **2006,** 72, 654-657.

47. Di Marco, A.; Gaetani, M.; Scarpinato, B., Adriamycin (NSC-123,127): a new antibiotic with antitumor activity. *Cancer Chemotherapy Reports. Part 1.* **1969,** 53, 33-37.

48. Dubowchik, G. M.; Padilla, L. M.; Firestone, R. A., An acid-cleavable linker stable at neutral pH that releases Doxorubicin at Lysosomal pH. *Bioorganic & Medicinal Chemistry Letters* **1993,** 3, 2843-2846.

49. Trail, P. A.; Willner, D.; Lasch, S. J.; Henderson, A. J.; Hofstead, S.; Casazza, A. M.; Firestone, R. A.; Hellstrom, I.; Hellstrom, K. E., Cure of xenografted human carcinomas by BR96-doxorubicin immunoconjugates. *Science* **1993,** 261, 212-215.

50. Aldersley, M. F.; Kirby, A. J.; Lancaster, P. W., Intramolecular Displacement of Alkoxide Ions by the Ionised Carboxy-group: Hydolysis of Alkyl Hydrogen Dialkylmaleates. *Journal of the Chemical Society, Perkin Transactions 2* **1974**, 1504-1510.

51. Kluger, R.; Lam, C.-H., Carboxylic Acid Participation in Amide Hydrolysis. External General Base Catalysis and General Acid Catalysis in Reactions of Norborneneyanilic Acids. *Journal of the American Chemical Society* **1978,** 100, 2191-2197.

52. Ikeura, Y.; Kurihara, K.; Kunitake, T., Molecular recognition at the air-water interface. Specific binding of nitrogen aromatics and amino acids by monolayers of Long-chain derivatives of Kemp's acid. *Journal of the American Chemical Society* **1991,** 113, 7342-7350.

53. Menger, F. M.; Ladika, M., Fast hydrolysis of an aliphatic amide at neutral pH and ambient temperature. *Journal of the American Chemical Society* **1987,** 110, 6794-6796.

54. Baldwin, B. W.; Hirose, T.; Wang, Z.-H.; Uchimaru, T.; Yliniemelä, A., New Kemp’s Diacid Derivatives Give Efficient Transport and Modifiable Selectivity for Alkaline Earth and Transition Metal Ions. *Bulletin of the Chemical Society of Japan* **1997,** 70, 1895-1903.

55. Guggenheim, E. A., XLVI. On the determination of the velocity constant of a unimolecular reaction. *Philosphical Magazine* **1926,** 2, 538-543.

56. Frost, A. A.; Pearson, R. G., *Kinetics and Mechanism*. Second ed.; John Wiley & Sons: New York, 1961.

57. Jencks, W. P., *Catalysis in Chemistry and Enzymology*. Dover Publications: New York, 1987.

58. Behme, M. T.; Cordes, E. H., Intramolecular Participation of the Amide Group in Ester Hydrolysis. *The Journal of Organic Chemistry* **1964,** 19, 1255-1257.

59. Kirby, A. J.; Lancaster, P. W., Structure and Efficiency in Intramolecular and Enzymatic Catalysis. Catalysis of Amide hydrolysis by the Carboxy-group of Substituted Maleamic Acids. *Journal of the Chemical Society, Perkin Transactions 2* **1972**, 1206-1214.

60. Denny, W. A.; Wilson, W. R., Bioreducible mustards: a paradigm for hypoxia-selective prodrugs of diffusible cytotoxins (HPDCs) *Cancer and Metastasis reviews* **1993,** 12, 135-151.

61. Katrizky, A. R.; Yao, G.; Lan, X.; Zhao, X., The Conversion of Secondary Amides into Tertiary Amides Using Benzotriazole Methodology. *Journal of Organic Chemistry* **1993,** 58, 2086-2093.

62. Levine, R.; Fernelius, W. C., The chemistry of the alkali amides. *Chemical Reviews* **1954,** 54, 449-573.

63. Challis, B. C.; Challis, J. A., Reactions of the carboxamide group. In *The chemistry of amides*, Zabicky, J., Ed. John Wiley & Sons: London, 1970; pp 731-857.

64. King, F. E.; Acheson, R. M., New potential chemotherapeutic agents. Part V. Basically-substituted isoalloxazines. *Journal of the Chemical Society* **1946**, 681-684.

65. Kelly, B. K. Studies of Potential Anti-Tumour Pro-Drug Systems. PhD Thesis, University of Waikato, Hamilton, 1997.

66. Atwell, G. J.; Wilson, W. R.; Denny, W. A., Synthesis and cytotoxicity of amino analogues of the potent DNA alkylating agent *seco*-CBI-TMI. *Bioorganic & Medicinal Chemistry Letters* **1997,** 7, 1493-1496.